MILITARY CAMP ACCOMMODATION COMFORT OPTIMIZATION

PhD doctoral thesis

Patonai Zoltán

Gödöllő
2023

Name of the Doctoral school: Doctoral School of Engineering Science

Discipline: Engineering Sciences

Head of Doctoral School: Prof. Dr. Kalácska Gábor
university professor, DSc
Hungarian University of Agriculture and Life Sciences,
Institute of Engineering

Supervisor: Dr. Géczi Gábor.
habilitated Associate Professor, PhD
Hungarian University of Agriculture and Life Sciences
Institute of Environmental Sciences

Associate Supervisor: Dr. Kicsiny Richárd
habilitated Associate Professor, PhD
Hungarian University of Agriculture and Life Sciences
Institute of Mathematics and Basic Science

. . . .
Approval of Head of Doctoral School   Approval of Supervisor

TABLE OF CONTENTS

1 INTRODUCTION

In my doctoral dissertation, I mainly rely on measurement results to investigate the effect of certain indoor air quality parameters in military camps on individual performance, as well as the effect of external environmental factors on the indoor air quality of camp comfort areas and rest areas.

1.1 Timeliness and relevance of the topic

Camp accommodation is one of the most important tasks for ensuring the basic purpose of the armed forces - in Hungary, the Hungarian Defence Forces. In peacetime, soldiers are stationed in barracks, where they can plan and organise their tasks necessary for the performance of their basic mission. However, it is easy to see that the actual execution of tasks directly corresponding to the basic mission from the barracks established, or effective preparation and training under realistic conditions, is not feasible in reality. For this reason, the use of Temporary Installations for military purposes is an essential service requirement.

For the provision of temporary facilities as military camps, the primary equipment currently used by the Hungarian Defence Forces to provide accommodation is tent and tent equipment. However, in line with the needs of the 21st century, the need for standard 20' containers is becoming more and more apparent. In accordance with international cooperation and based on the experience gained in the last 20 years, there is a trend towards the replacement of the tented accommodation planned for the provision of permanent duty assignments by the use of containers as temporary facilities. Obviously, both solutions have advantages and disadvantages, depending firstly on the planned period of use of the Temporary Facility - and the time available for installation and preparation, and secondly on the nature of the task. In order to determine the reasonable and sustainable energy requirements for camp operation, it is necessary to assess the internal air conditions under which the performance of the installed stock can be maintained at the highest value.

In the light of the experience of the past 20 years, and based on my research, the concept of Provisional Installations as military camps needs to be rethought. Particular attention should be paid to the planning of camp operations. The basic design data and requirements that help to build temporary infrastructures have so far generally been based on empirical data,

which, when examined, are no longer valid. Recognising this, there is a need for a comprehensive review of temporary facilities in order to establish a sound basis for the design of today's infrastructure. In line with the environmental engineering practices of the 21st century, energy efficiency and recyclability are increasingly required for military installations.

1.2 Objectives to be achieved

My objective is first of all to observe the temperature evolution in the accommodation enclosures of military camps using ISO 20' standard containers (hereafter ISO 20' containers), controlled by the Internal Air Quality (hereafter IAQ), based on subjective thermal sensation.

Secondly, to assess the impact of the external environmental parameters according to the weather conditions in Hungary, the variation of the indoor air quality of the different building materials at rest, the thermal comfort and the air components/pollutants.

Finally, I aim to investigate the effect of elevated carbon dioxide concentrations in the IAQ of the placement ranges on the soldier's individual combat, or more specifically situational shooting performance.

2 MATERIALS AND METHODS

In this chapter, I describe the operation of the experimental areas and the equipment and measuring systems used in the research work, as well as the methods and correlations of the measurement series. Since I have carried out a series of measurements at several sites using different methods, I will present their construction, instrumentation and operation separately.

2.1 Internal temperature measurements under field conditions

The comfort tests were carried out in an operational facility, by monitoring the indoor air quality of the Border Guard Bases' accommodation areas in 4 locations along the southern border of Hungary.

2.1.1 Description of the experimental areas

The facility under consideration is a relocatable complex of buildings with a total capacity of 150 people. The dimensions and advantages of the containers comply with the ISO standard for 20-foot office containers, designed and constructed according to the type design of Mobilbox Ltd (http://mobilbox.hu). As a base, the compacted crushed stone bed is leveled and supported using 3 concrete walkway footings at 6 points. The placement perimeters of the border guard bases are 30 cubic meters each, which can accommodate 4 persons. The structure is based on a solid frame and removable panel system, the dimensions of which are shown in Table 1.

Table 1, ISO 20' container dimensions

container dimensions (ISO Standard 1161)	Length	Width	Height
Outside dimensions	6.055 mm	2.435 mm	2.591 mm
	(+ 0,-6 mm)	(+ 0,-5 mm)	(+ 0,-5 mm)
Inside dimensions	5.855 mm	2.231 mm	2.329 mm
	(+ 0,-6 mm)	(+ 0,-5 mm)	(+ 0,-5 mm)

The external wall element is made up of 3 layers, with the following layering scheme:

1. Outer casing: 0.5 mm steel sheet, galvanised, painted, with ribs,
2. Insulation: 60 mm thick mineral wool in wooden frames,
3. internal cladding: 10 mm laminated wood chipboard with wood grain (maple colour), quality class P2 (EN 312) E1 (EN 13986).

The corner posts are insulated with rock wool to reduce thermal bridges.

2.1.2   *Experimental equipment and measurement series*

For temperature and humidity measurement and data collection at the Border Guard Bases, I used an Ebro sensor and data logger, which included an EBI 300-TH measuring data logger with a THP 400 external capacitive humidity sensor (Ebro, Ingolstadt, Germany). The instrument can record data over a measuring range of -30 °C to +60 °C with an accuracy of ±0.5 °C. The manufacturer certifies that the instruments comply with GMP-/HACCP/IFS regulations.

Remote EBI-300TH measuring/data logging instruments record the humidity in the bedroom and the internal temperature, which is controlled by the occupants according to their needs. The temperature setting is a subjective value that depends on the thermal sensation of the individual placed and the individuals in the enclosure, so our aim was to record data as widely as possible. Measurements were carried out at border protection bases in summer 2019 (hot) and winter 2019-2020 (cold) and in winter and spring 2022. The broad scope of data collection is helped by the fact that there is a 2-week rotation of soldiers serving at the border protection bases, which allowed for a wider range of users to collect the recorded data. As a result, the winter measurements were recorded in 3 grid circles over 24 weeks (12 shifts), with 36 different rest circle personnel - i.e. broken down into separate individuals; in total, one company of sub-unit soldiers - subjectively set to different air temperature settings.

The measurements primarily recorded data on indoor humidity in the sleeping quarters and the indoor temperature set by the soldiers, but in parallel I also recorded data on the expected indoor thermal comfort in the office space. When evaluating the internal temperature data for the accommodation circles and office containers, it should be borne in mind that soldiers are basically in the office container during working hours, which is usually between 07.00 and 17.00.

The results of the summer measurement were recorded in 4 grid loops until 31 July 2019. During the winter months, I continued to measure the subjective set internal temperature, supplemented by measuring the external temperature. The results of the outdoor temperature measurements were also recorded with an EBI-300TH measuring data logger. The recorded external temperature data is of excellent use in selecting a single interval to be investigated and provides a basis for filtering the recorded seventy thousand measurements. During the first winter period, the data loggers were deployed

on 13 November 2019- 13 November 2020 and recorded indoor temperature and relative humidity data on average until mid-February 2020 with quarterly sampling. The continuation of the measurement tasks was not allowed by the COVID epidemic control regulations, which allowed me to continue recording data in 2022.

In the grid cells, carbon dioxide concentration variations were measured separately using an ALMEMO 2590 measuring and storage unit with attached sensors (Ahlborn, Illmenau, Germany). In addition, I used indoor air quality measurement and data recording devices of the type Pyle PC02 MT05 and Wohler CDL 210 (Bad Wünnenberg, Germany), the description and manufacturer's data of which are described in detail in chapter 3.2. Due to the different handling and use of the instruments, it was only possible to make these measurements for a single day, and it was not possible to collect data over weeks or months. However, as I have described in the literature, there are a similar number of empirical values available to investigate the changes caused by people living in comfort rooms and the effects on humans during fruit storage. The increase in CO_2 concentrations caused by the respiration of fruit in a test room by an appropriate amount of fruit is similar to the change caused by human respiration, so the equations used for indoor air quality indicators can be used in this area if the respiration of the fruit/vegetable is known or can be measured. Taking advantage of this similarity, we stored vegetables and fruits for 4 to 10 days in the border base food storage facility, where we were also able to continuously monitor the air temperature, humidity and CO_2 concentration of the storage (also an ISO 20' container) under real-time continuous operation, subject to COVID regulations.

2.2 Different models set up in a civil engineering laboratory

At the Hungarian University of Agricultural and Life Sciences, Laboratory of Civil Engineering and Environmental Engineering, I have set up several experimental spaces to model the campsite environment.

For the determination of temperature, humidity, carbon dioxide concentration, solar radiation intensity, wind speed, wind direction and atmospheric pressure values representing the outdoor conditions and for the storage of the measured values I used an ALMEMO 2590 measuring and data storage unit and its connected sensors (Ahlborn, Illmenau, Germany). In addition, I used indoor air quality measurement and storage devices of the type Pyle PC02 MT05 and Wohler CDL 210 (Bad Wünnenberg, Germany) equipped with a digital carbon dioxide air pollution sensor. The devices are

universal indoor air quality (IAQ) meters that record air carbon dioxide concentration, temperature and humidity. The gas measurement technology is non-dispersive infrared detector (NDIR), particle measurement 2.5/µm particle size, CO_2 measurement range: $0 \sim 9999$ ppm ± 70 ppm. Temperature measurement range $-10 \sim 70$ °C with ± 0.3 °C accuracy. Humidity measurement range: $0\% \sim 99.9\%$ (relative humidity) with an accuracy of $\pm 3\%$. (Global) solar radiation was measured with a Theodor Friedrichs 6003.3000 BG sensor with an accuracy of 30 W/m2, wind speed was measured with a Thies Clima 4.3519.10.000 with an accuracy of 0.5 m/s. Power supply: 110/220 V AC / DC 5 V USB wall adapter. For a valid comparison of the data recorded with the different measuring instruments, a calibration measurement was performed for the certified ALMEMO type measuring instrument.

2.2.1 ISO 20' container model, IAQ measurements

In relation to the ISO 20' containers used for the construction of bases for the protection of the southern border of Hungary, as a test of the behaviour of the building material itself under environmental influences, I modelled with an ISO 10' container set up in the building engineering laboratory (Fig. 1).

Figure 1. Model of a container building in the university laboratory

The physical characteristics of the structural elements of the ISO 10' container are identical to those of the ISO 20' containers in the military camps set up, the only difference being that the longitudinal side of the ISO 10' container is only 3 m, compared to the ISO 20' container, where it is 6 m. The orientation of the container is the same as described above, with the

difference that the entrance door of the container is in this case oriented in the D direction. The solar collector mounted on the top of the container did not work at all during the measurements, i.e. it did not heat the inside of the container either directly (by space heating) or indirectly (by producing domestic hot water). The observed temperatures were measured with K-type thermocouples (u_T = 1 °C with an average uncertainty). The (global) solar radiation was measured with a Theodor Friedrichs 6003.3000 BG sensor (u_I = 30 W/m^2 with an average uncertainty) in the plane of the solar collector, south facing, at an inclination of 40°. Wind speed was measured using a Thies Clima 4.3519.10.000 instrument (u_v = 0.5 m/s average uncertainty). Measurements (I, T_k, v and T_b) were taken at 30 s intervals (Δt = 30 s).

The second series of measurements was carried out in the year 2021, between March 10 and October 10, 2021, in a model built with an ISO 10' container. I measured the internal temperature and its influencing parameters in order to determine the energy transport required to achieve the desired IAQ.

Table 2, Data measured on the model set up in the laboratory:

	Measured data	mark	unit of measurement
1	Inside temperature	T_b	[°C]
2	Tent inside temperature	T_s	[°C]
3	Outside temperature	T_k	[°C]
3	Global radiation intensity	I	[W/m^2]
4	Wind speed	v_{sz}	[m/s]
5	Wind direction	WD	-
6	Container inside atmospheric pressure	p_b	[mb]
7	Outside atmospheric pressure	p_k	[mb]
8	Container inside air carbon dioxide concentration	CO_2	[ppm]

The data presented in Table 2 were measured twice every minute. The measured value of T_b is for identification and comparison purposes only, i.e. no thermal measurements were made in this case. The initial value of the

measured $T_{b(0)}$ is entered as a condition in the models. The tests were performed in 24-hour units with five replicates.

Carbon dioxide variation in a series of measurements in ISO 10' containers, simulated by myself/ourself (research and subject leaders) as a test subject with actual occupancy and observed the carbon dioxide concentration rise time for several (2-3) persons. In a second set of measurements, I measured the rise time of carbon dioxide concentrations produced by 1 person and 2 persons primarily in order to be able to adjust the parameter for modelling the number of occupants as a pollutant point source to be adjusted by external addition (CO_2 cylinder). In a third series of measurements, I calibrated the artificially adjusted pollutant point source by different settings of the CO_2 bottle reducer, comparing the formation and rise time of carbon dioxide concentrations produced by 1, 2 and 3 individuals with the previously measured ones. I compared these measurements with the amount of carbon dioxide produced by human respiration as described in the literature, physiological effects of carbon dioxide, and with the mathematical model described in the literature, fresh air demand (7).

Taking advantage of the finding that the increase in CO_2 concentration caused by fruit respiration is similar to the change caused by human respiration, I also took measurements in the food storage area of the border base, observing changes in air temperature, humidity and carbon dioxide concentration.

The primary objective was, of course, to monitor the CO_2 concentration, which was influenced not only by the internal source (post-ripening and respiration of vegetables and fruits) but also by the fresh air entering the container (evaporation-storage and filtration). Increased CO_2 concentrations were observed after only 1 hour, but did not rise above a certain level without opening. With the operation of the camp kitchen, the regular and continuous unloading and loading of the food storage and the natural filtration of the container, the expected increase in CO_2 concentration did not occur. I found that during short term storage, the carbon dioxide concentration does not reach the level necessary to slow down metabolic processes, but the studies on the subject presented in the literature on carbon dioxide effects in technological installations usually investigate changes during long term storage, i.e. longer than 1 week, e.g. grapes have been tested for 1 month, and experiments with apples have been carried out for several months, up to half a year. In order to compare my research with similar studies, I made observations in the laboratory, modelling the

behaviour of closed storage for more than 24 hours. In a container set up in the laboratory area, I carried out tests with fresh Idared (Malus domestica) apples from a Hungarian grower in order to obtain data on the variation of the CO_2 concentration in the air, without opening the container door on a daily basis.

Later, I achieved carbon dioxide load reduction by introducing food-grade carbon dioxide. These measurements are identical to the measurements made in the comfort room, given the identity of the point source. I also used the calibration of the reductor settings described in the previous chapter to model the respiration of the fruit. However, the data and results obtained from simulation observations with carbon dioxide cylinders will be presented later in this thesis for the sole purpose of evaluating the optimal placement comfort.

2.2.2 Model M63 unit tent, comparative measurements

To model the camp built with tent material, a tent of M63 design was also set up in the area of the building engineering laboratory from the Hungarian Defence Forces' stock, as already shown in the background of Figure 1. The dimensions of the M63 tent are shown in Table 3, marked as in Figure 2.

Table 3, 63M military tent main dimensions and weight data

size marked in Figure 2	identification of structural size	distance [cm]
1	Width at ground level	500
2	Roof width	400
3	Length (depth)	414
-	Folding length (as additional tent)	340
4	Peak (ridge) height	268
5	Side height	172
6	Entrance width	140
-	Entrance height	172

The tent has a floor area of 17 m², without vestibule, tarpaulin weight 31 kg, tent frame and accessories 55 kg.

Figure 2. 63M military tent main dimensions and weight data

When setting up the tent, I took care to ensure that both the tent and the ISO 10' container were equally exposed to the external environment. I placed it with a similar S-SW orientation, and even though the windows were oriented N-NE, I set the sunlight entering through the windows to have the same window area for equality.

The measurements were carried out between 10 March 2021 and 10 October 2021, using the ALMEMO measuring instrument in the ISO 20' container, also described in chapter 3.2, with a measurement every 30 seconds ($\Delta t = 30$ s). The temperature in the tent was measured with a K-type thermocouple ($u_T = 1$ °C average uncertainty) connected via an extension to the ALMEMO 2590 measuring and storage unit in the ISO 10' container, ensuring the unambiguous comparability of the data recorded with the calibrated instrument

2.2.3 Physics-based mathematical model

To determine the internal temperature, the correct use of the mathematical model requires the identification of the internal temperature, which is fundamentally influenced by the ambient external temperature, the internal heat source such as the number of people in the enclosure and the heat they emit, and the external factor of wind speed, which increases the convective heat dissipation of the container and the natural filtration of the internal space. As an environmental effect, the intensity of the solar radiation is of course also responsible for the heat input into the system.

The physically based linear mathematical model of the placement envelope, hereafter referred to as the physics-based model, is as follows:

$$T_b(t) = T_b(t-\Delta t) + k_I \, I(t-\Delta t) \, \Delta t + (a \, v_{sz}(t-\Delta t) + b) \, (T_k(t-\Delta t) - T_b(t-\Delta t)) \, \Delta t \quad (2)$$

14

k_I, **a** and **b** are the constant parameters to be specified in the model. The modeled value of T_b is $t = \Delta t, 2\Delta t, 3\Delta t,...$ shall be determined according to equation (2). The measured value of T_b at time $t = 0$ is used as the initial condition.
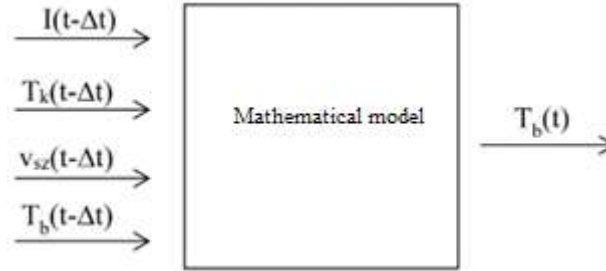

Figure 1. Block diagram in terms of inputs and outputs

Figure 3 shows the block diagram of the physics-based model in terms of inputs ($I(t-\Delta t)$, $T_k(t-\Delta t)$, $v_{sz}(t-\Delta t)$, $T_b(t-\Delta t)$) and output ($T_b(t)$). The parameters k_I, **a** and **b** (31), whose identification was carried out in three steps as follows:

First, on day 6 of the identification, I selected the measured data when the wind speed was continuously zero for at least 5 min and the solar irradiance was less than 10 W/m² (i.e., the next section, MLR model - case A1). In this case, the effects of **a** and k_I are negligible (since $\mathbf{v} \approx 0$ m/s and $\mathbf{I} \approx 0$ W/m²). Under these boundary conditions, **I** identified the value of **b** as **b** = 0.0000206 [1/s], since the time average of the absolute difference between the modelled and measured internal temperature, i.e. the mean of the absolute error, is minimal with this value for these periods.

To check the identification of models (both physics-based and MLR mathematical models) and to evaluate the validation, I used the relative error (h_T) over the measurement range (Kline and McClintock 1953, Kicsiny 2017, Kicsiny 2018, Géczi et al 2019).

$$h_T = \frac{\overline{H_T}}{T_{meas\_max} - T_{meas\_min}} \, [\%] \tag{3}$$

where:

- $\overline{H_T}$ – modelled internal temperature mean error,
- T_{meas} – measured inside temperature,
- T_{mod} – modeled inside temperature,
- **n** – number of measurements.

15

I calculate the modelling mean error ($\overline{H_T}$) as the average of the differences between the measured temperature (T_{meas}) values and the modelled temperature (T_{mod}) values:

$$\overline{H_T} = \frac{|T_{meas\_1} - T_{mod\_1}| + |T_{meas\_2} - T_{mod\_2}| + \cdots + |T_{meas\_n} - T_{mod\_n}|}{n} \quad (4)$$

Note: in Section 2.2.5, I use the same procedure to calculate the modeled concentration error for the indoor air carbon dioxide content, identifying the mean absolute error ($\overline{H_T}$), with T_{meas} replaced by - K_{meas} as the measured indoor carbon dioxide concentration, and T_{mod} replaced by - K_{mod} as the modeled indoor carbon dioxide concentration.

The second step in the identification of the physics-based model is that, since I have already selected the data from the 6 days of the identification period when I measured wind speed continuously at zero for at least 5 minutes (including the periods of step 1 above). That is, in these cases, the effect of wind is negligible (since $v \approx 0$), but I now consider the period where the global irradiance $I > 10$ W/m^2 (i.e. the same as in the MLR model - case 'B', described in more detail in the next section). So, in the present case, the value of **a** is still negligible, since $v \approx 0$ m/s and, when calculated with the already identified **b**, I have identified the value of k_I as $k_I = 0.00000047$ [m^{2}K/J], since the mean of the absolute error is minimal with this value for these identification periods.

Finally, I identified the '**a**' value for the entire 6 days of identification (including the periods of steps 1 and 2 above) which I set to $a = 0.000028$ [1/m], since the mean absolute error is minimal with this value for these periods (in addition to the **b** and k_I values already identified).

To check the expected value of the CO_2 concentration by calculation, I did not construct my own physics-based mathematical model as I did for the indoor temperature check presented above, but used the mathematical model presented by HERCZEG et al (2000), which is a suitable and accepted model for calculating the expected value of the concentration in the indoor air due to the effect of different pollutant point sources.

2.2.4 *MLR model of container inside temperature*

The inputs to the MLR-based model to be developed for internal temperature modelling are derived from the appropriately chosen values of **I**, T_k and V_{sz} similar to the block diagram presented for the physics-based model (Figure 4). The output is also the same, i.e. derived from appropriately chosen values of T_b.

16

The placement container is represented in the MLR-based modelling as a black-box model. It is easy to see that within the overall MLR-based model, separate sub-models need to be created in order to model temperature well under significantly different operating conditions. Basically, the sign and/or intensity of the internal temperature change is different when solar radiation is negligible and different when the effect of global radiation cannot be neglected.

Based on our observations, three basic operational cases can be distinguished in a day, as shown in Figure 4:

- **Case A1** covers the period from the beginning of the day until the first time when the global irradiance does not exceed 10 W/m^2.

- **Case B** covers the period from the end of Case A1 to 21:00 h (the part of the year currently under consideration).

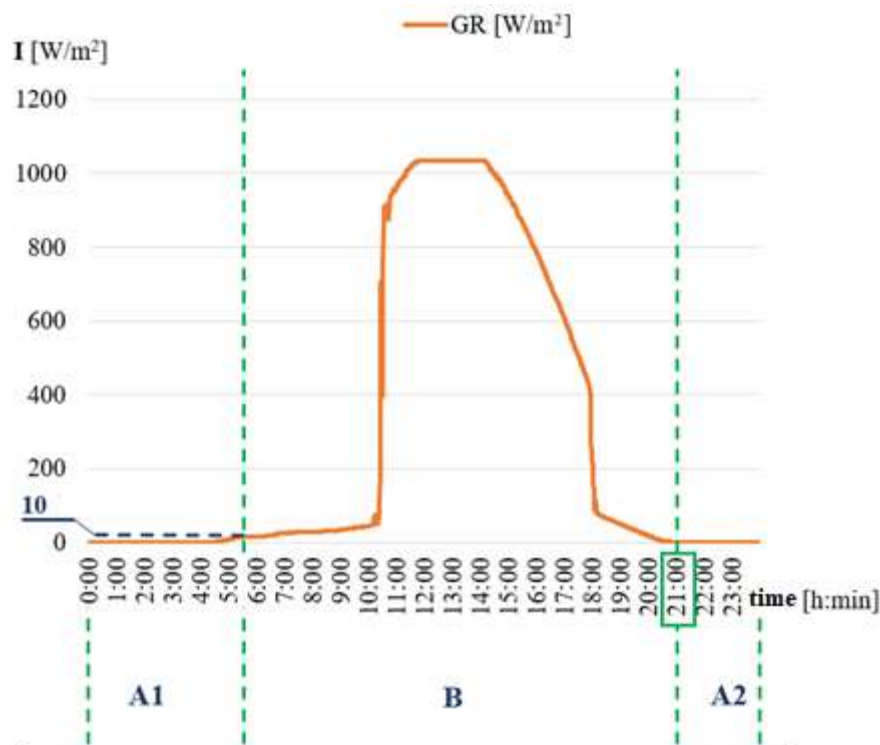- **Case A2** covers the period from 21:00 until the end of the day.

Figure 2. Solar radiation and operational cases

The block diagram illustrated in Figure 3 also applies to the MLR-based model in terms of inputs and outputs. In line with the above, separate MLR-based sub-models have been created for each of the operational cases for better modelling accuracy. Equations (5) to (7) represent the submodels as linear relationships:

A1 case: $T_b(t) = c_{I,A1}I(t - \Delta t) + c_{k,A1}T_k(t - \Delta t) + c_{v,A1}v(t - \Delta t) + c_{b,A1}T_b(t - \Delta t)$ (5)

B case: $T_b(t) = c_{I,B}I(t - \Delta t) + c_{k,B}T_k(t - \Delta t) + c_{v,B}v(t - \Delta t) + c_{b,B}T_b(t - \Delta t)$ (6)

A2 case: $T_b(t) = c_{I,A2}I(t - \Delta t) + c_{k,A2}T_k(t - \Delta t) + c_{v,A2}v(t - \Delta t) + c_{b,A2}T_b(t - \Delta t)$ (7)

$c_{I,A1}$, $c_{k,A1}$, $c_{v,A1}$, $c_{b,A1}$, $c_{I,B}$, $c_{k,B}$, $c_{v,B}$, $c_{b,B}$, $c_{I,A2}$, $c_{k,A2}$, $c_{v,A2}$, $c_{b,A2}$ are the constant parameters to be identified in the model. The modelled value of T_b is $t = \Delta t$, $2\Delta t$, $3\Delta t$,... (The measured value of T_b at time $t = 0$ is used as the initial condition.)

2.2.5   2.2.5 MLR model of IAQ carbon dioxide concentration

The inputs to the MLR-based model to be developed for modelling carbon dioxide concentrations are derived from the appropriately chosen values of K, ΔT and V_{sz}. The output is derived from appropriately selected values of K_b.

The above marks:

- $\dot{K}$ – carbon dioxide inside point source,
- ΔT –difference between outside and inside air temperature,
- V_{sz} – wind speed,
- K_b – inside air carbon dioxide concentration.

Initial observations were for Δp, i.e. the difference between atmospheric pressure in the interior and exterior, but in keeping with the research topic, military reconnaissance data such as climate and meteorological data, and the previous result, i.e. the interior temperature model, I chose ΔT as the input to the MLR-based model of the interior concentration change. I assumed that, based on the gas laws at constant volume, $p_1/p_2 = T_1/T_2$. I verified my assumption with measurements, which I present in the results, section 3.2.3 (Figures 24, 26, 28, 30).

In the MLR-based model, as in the previous chapter where I modelled the internal temperature change, only the internal air concentration rate $K_{b(t-\tau 1)}$ can play a role, where the positive constant $\tau 1$ represents a time lag. Similar considerations apply to K, V_{sz} and ΔT due to their limited propagation velocity, so that the previous values of $K_{(t-\tau 1)}$, $V_{sz(t-\tau 1)}$ and $\Delta T_{(t-\tau 1)}$ may play

an input role in the development of the internal air concentration $K_{b(t)}$. (Here, the time lags of K, V_{sz} and ΔT are assumed to be the same at $(\tau 2)$ for simplicity.) Of course, the corresponding prior value of the indoor air concentration may also influence the value of K_b, and essentially acts as the initial value of the MLR-based model at $(t-\tau 2)$. In the identification of the MLR-based model, when measured values of $_{Kb}$ are available, the measured value of $K_{b(t-\tau 2)}$ (i.e. $K_{b,meas(t-\tau 2)}$) will be used as this initial value. In the validation of the MLR-based model, the previously modelled value of $K_{b(t-\tau 2)}$ (i.e. $K_{b,mod(t-\tau 2)}$) will be used as this initial value when modelling K_b - t at time t (i.e. $K_{b(t)}$). Measured values of the inputs $K_{b(t-\tau 1)}$, $K_{(t-\tau 2)}$, $V_{sz(t-\tau 2)}$ and $\Delta T_{(t-\tau 2)}$ are available for both identification and validation.

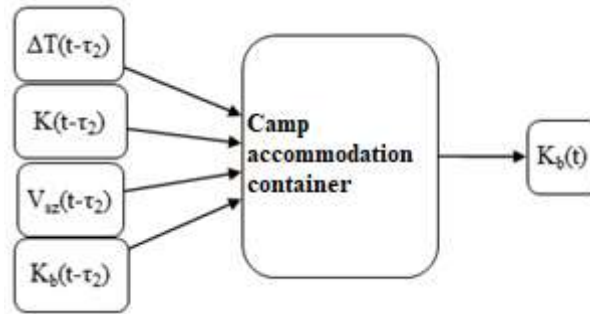The block diagram of the MLR-based sub-model is shown in Figure 5.

Figure 3. Block diagram of the MLR-based model

If the model is considered as a black box, it is recognised that the different sub-models, i.e. the parts of the MLR-based model to be developed, need to be identified under significantly different operating conditions. For example, the container behaves quite differently when the ambient wind speed at the surface is increased (v > 2 m/s) or decreased (2 m/s > v). Under the same conditions, including ambient wind speed, the internal air pollution concentration of the container, i.e. K_b, increases much more intensively when it starts to increase due to the presence of an internal point source, and in the meantime the room filtration decreases.

The MLR-based model consists of the following linear mathematical equations:

$$K_{b,mod(t)} = c_K, \dot{K}(t-\tau 2) + c_{\Delta T}, \Delta T(t-\tau 2) + c_V, V_{sz}(t-\tau 2) + c_{Kb}, K_b(t-\tau 2) + c \quad (8)$$

The constant parameters to be identified are c_K, $c_{\Delta T}$ c_V, c_{Kb} and c. The time points for the $\tau 2$ measurements are $t = 0, \tau 2, 2\tau 2, 3\tau 2$. The value of the modelled K_b (i.e. $K_{b,mod}$) is determined at time points $t = \tau 1, 2\tau 1, 3\tau 1,...$

19

using equation (8). (I use the measured value of K_b at time point $t = 0$ as the initial condition.) In line with the above, for better modeling accuracy, the MLR-based submodels are identified separately for each operational case, according to the fact that the value of K_b starts from the same value as fresh air, continuously monotonically increasing until a first 3 min measurement data average (to be determined depending on the sensitivity of the measuring instrument) of 15 ppm carbon dioxide concentration drop is observed.

2.3 Measuring the impact of CO_2 exposure on military capability

I measured the military capability with a basic situational test at the HDF Nagysándor József 51st Signal- and Command support Brigade in Székesfehérvár. The situational exercise was carried out at the barracks' 4-post pistol range, a series of experiments; 1 day / 3 groups.

In order to measure the effect of carbon dioxide on the CO_2 concentration in the modelled housing envelope, I used the ALMEMO instrument described above, supplemented with Pyle PC02 MT05 and Wohler CDL 210 measuring and recording devices, to ensure the instrumentation for continuous monitoring of the indoor air CO_2 concentration required by the protocol used for the live-fire experiment.

2.3.1 Description of the experimental area

To carry out the situational exercise, I have defined a distance of 80 meters (Figure 6), according to the conditions and equipment of the firing range, in which the soldier has to cover 59 meters until the fire is released, and at a distance of 15 meters he has to fire 5 targeted shots at a circular breaststroke.

Figure 4. Outline of the implementation of situational shooting

The containers used for modelling the field perimeter of the shooting range were provided by the Hungarian Defence Forces, and therefore they are identical to the structural elements of the ISO 20' containers used in the bases of the southern border defence of Hungary.

2.3.2 Description of the measurement series

I measured military capability with a basic situational test. In the situational exercise tested, subjects are spending their free time (or doing sedentary work) in a camp accommodation area when the camp is under attack. A terrorist group blows through the camp wall with a suicide vehicle equipped with a bomb, in which area armed assailants enter the camp area. When the camp is attacked, an "Intruder Alert" is ordered, which requires the soldier in the placement perimeter to rush to the designated bunker.

Between the emplacement perimeter and the bunker, after a distance of 59 meters from the perimeter door (Figure 6), the soldier encounters an armed terrorist who must be defeated with his self-defence handgun in order to successfully complete his designated bunker activity as rehearsed in the field alert. He must fire 5 shots to destroy the bunker, with the time of execution being recorded by the last shot fired. After the execution time has been recorded at all firing positions, the location of the hits on the firing points is accurately recorded.

After a briefing on the rules of engagement, weapons familiarisation and practice, the unloaded shooting was carried out. The soldier is in the open air for a minimum of 70 minutes, where the CO_2 concentration is between 400 and 450 ppm. When the "intruder alert" was sounded, the tested group of 4 men simultaneously moved independently to the firing range and independently engaged the target with 5 aimed shots. After the execution of the unloaded firing, the soldier retreats to the prepared camp rest container where the internal air CO_2 concentrate is set to the load condition.

$$3000 \text{ ppm} < k_b < 4000 \text{ ppm} \tag{9}$$

When maintaining a load IAQ condition, particular attention should be paid to the protocol, developed as described in the literature, to stop the experiment when a maximum concentration of 4500 ppm is reached, subject to the standard value for the air quality of carbon dioxide in the workplace (5000 ppm = MAC value).

In the next phase of the measurement series, the soldier spent 70 minutes in the field in a loaded condition and then repeated the situational shooting on "intruder alert". He then retreated again to the prepared field enclosure where, after another 70 minutes of loading in the set CO_2 concentrate, he performed the second loaded firing.

21

The carbon dioxide level was set in a confined space following the protocol described in the literature (ALLEN 2015) to ensure the safety of the participants, where CO_2 levels were monitored in real time in the test rooms using three different calibrated meters. A technician seated next to the CO_2 shut-off valves monitored the CO_2 concentration throughout the test period, and the meter readings were continuously monitored by an external helper through the window from outside. The protocol was to stop the test immediately if CO_2 concentrations exceeded predetermined thresholds, which I defined as 4500 ppm, i.e. below the occupational health limit, 90% of it. The experiment was ensured by 2 senior EC medical officers from the MH EC staff (traumatology assistant and anaesthesiology assistant) and 1 senior safety and occupational health engineer.

2.3.3 Methodology for the evaluation of results

The shooting is evaluated by recording the result of the shooting achieved by each soldier, where the following perimeters are recorded:

- hit score achieved [**KP**]
- average distance of hits from the middle hit point [**SD**]
- the time needed for implementation [**t**]

The hit score is calculated as the sum of the hit scores of the 5 shots fired in each situational shooting:

$$KP_{sum}=KP_1+KP_2+KP_3+KP_4+KP_5 \tag{10}$$

The hit score was evaluated using the loaded/unloaded ratio, which means that the soldier's performance is not reduced - i.e. 100% - if he achieves at least as many rounds in the loaded shooting task as in the unloaded task at baseline. If no hits of value are scored when fired from a CO_2-loaded internal environment, then 0%.

$$\eta_{KP} = \frac{KP_{(loaded)}}{KP_{(unloaded)}}, \tag{11}$$

To calculate the average distance of hits from the centre hit point, the first step is to determine the central hit point [CHP] itself. As a first step in determining the central hit point, the 5 hits were numbered according to their distances from the central of the stone slab and, by placing the stone slab in the coordinate system, the hit point Sn was identified by coordinates (xn;yn), according to which the hits were registered in sequence:

$$S1_{(x1;y1)}, S2_{(x2;y2)}, S3_{(x3;y3)}, S4_{(x4;y4)} \text{ és } S5_{(x5;y5)} \tag{12}$$

22

By connecting the first two matches identified in the sequence, halving their distance, I connect the third match, dividing its distance by a third, connecting the fourth match by a point, dividing its distance by a quarter, connecting the fifth match and dividing its distance by a fifth, I get the Central Hit Point [**CHP(x_k;y_k)**].

After determining the central hit point by measuring the distance of each shot and averaging it, I get the standard deviation for the 5 hits.

$$SD = \frac{(CHP_k - s_1) + (CHP_k - s_2) + (CHP_k - s_3) + (CHP_k - s_4) + (CHP_k - s_5)}{5} \quad (13)$$

After a single situation, I identify the average distance of each fighter's hits from the center of variance, i.e., the standard deviation, with the loaded/unloaded ratio, similar to the evaluation of the hit score. Accordingly, there is no reduction in the soldier's performance - i.e. 100% - if the standard deviation is no greater during loaded shooting than during the baseline condition, i.e. the unloaded task. If, on initiation from a CO_2 - loaded internal environment, no appreciable hits are achieved, then 0%.

$$\eta_{SD} = \frac{SD_{(loaded)}}{SD_{(unloaded)}}, \quad (14)$$

I recorded the time required for execution in [t] seconds (s). The recorded execution time represents the time required for the activity that starts with the sounding of the "intruder alarm" and ends with the firing of 5 targeted shots and the subsequent concealment of the weapon, at the completion of which the soldier takes 1 step back from the firing position indicating that the target has been engaged.

The change in execution time of situational shooting gave the most significant measure of the change in performance indicators, which I also evaluate by the loaded/unloaded ratio, according to which the soldier's performance does not decrease - i.e., 100% - if he can perform his task in at least the same time during loaded shooting as in the baseline condition, i.e., the task performed without load. However, in this case, I have defined a time constraint, i.e. 0% execution time performance if it takes double the time to resolve the situation when moving from a CO_2 - loaded internal environment.

$$\eta_t = 1 - \frac{t_{(loaded)} - t_{(unloaded)}}{t_{(unloaded)}}, \quad (15)$$

In order to compare the results of the presented loaded and after 70 min of shooting at carbon dioxide concentrations above 3000 ppm, I performed two-sample t-tests and checked that the difference between the recorded results of the shooting in the carbon dioxide loaded condition was significant.

$$t := (t_{n+m-2}) := \frac{\bar{x}-\bar{y}}{\sqrt{(n-1)\sigma_n^{*2}+(m-1)\sigma_m^{*2}}} \sqrt{\frac{nm(n+m-2)}{n+m}} \qquad (16)$$

The results recorded during the experimental situational shooting to measure the performance of the military skill were evaluated separately for the hit score [KP], mean distance from the mean of dispersion [SD] and time to execution [t] as described above. To be able to reproduce the variation in combat capability in general, a unit efficiency characteristic is required [η_H].

I identify the definition of the efficiency characteristic of situational shooting in a single unit with the load/unload ratio. I consider both the ability to concentrate, which I identify with the average distance from the mean hit point of the shot, i.e., the standard deviation, and the hit score, and the speed, i.e., the time to complete the situational task. Accordingly, the soldier's performance is not reduced - i.e. 100% - if he can perform the task in at least the same amount of time and with the same accuracy during loaded shooting as in the baseline condition, i.e. without the load.

$$\eta_H = \frac{\eta_{(KP)} * \eta_{(t)} + \eta_{(SD)} * \eta_{(t)}}{2}, \qquad (17)$$

In this case, too, a time constraint must be taken into account, according to which 0% of the soldier's situational firing performance is required if, starting from a CO_2-loaded indoor environment, double the time is needed to resolve the situation.

3   RESULTS

In this chapter, I present the results of a series of measurements at different locations and the mathematical models generated using multiple linear regression (MLR). The validation results for the two different IAQ parameters are presented in separate subsections.

3.1   Investigation of indoor air quality in a storage container

In this chapter I present my measurements at the border protection bases along the southern border of Hungary. I started measuring the internal temperature, which was set by the soldiers based on their subjective perception of temperature, in addition to the external temperature in the winter months of 2019 - 2020.

I highlight January 2020 as the coldest period in the measurement range. The coldest temperature measured was -8.6 °C on 24 January 2020 at 8 a.m. The warmest temperature measured was 10.5 °C on 11 January 2020 at 2 p.m. and 15.7 °C at the end of the month on 31 January 2020 at 3 p.m. The average outside temperature was 0.2 °C (Figure 7). The average indoor temperatures measured in the dwelling units ranged between 23 °C and 28 °C, with an overall average of 24.5 °C as the subjectively set or expected indoor temperature. The indoor relative humidity results were measured between 32% and 42%, with an overall average of 37% as the established indoor humidity. It is important to consider the period of time I am testing the indoor air temperature set by the individual to achieve a controlled, comfortable thermal comfort.
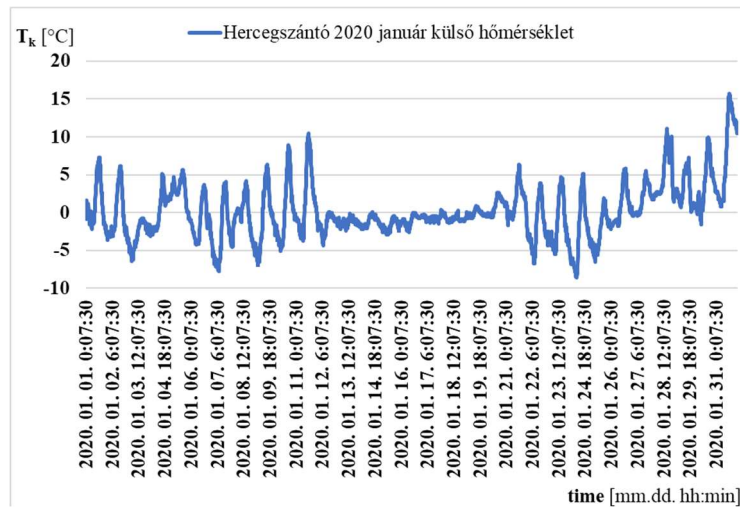

Figure 5. Hercegszántó HVB, outdoor temperature in January 2020

The soldiers serving at the Border Guard Bases carry out their duties according to a daily schedule. They use their quarters during rest periods and stay at their duty stations when on duty. Based on the data recorded in the enclosure No 5 (Figure 8), the data must be sorted according to the daily schedule, because in this way we can record values specifically set according to the individual temperature of the soldiers.
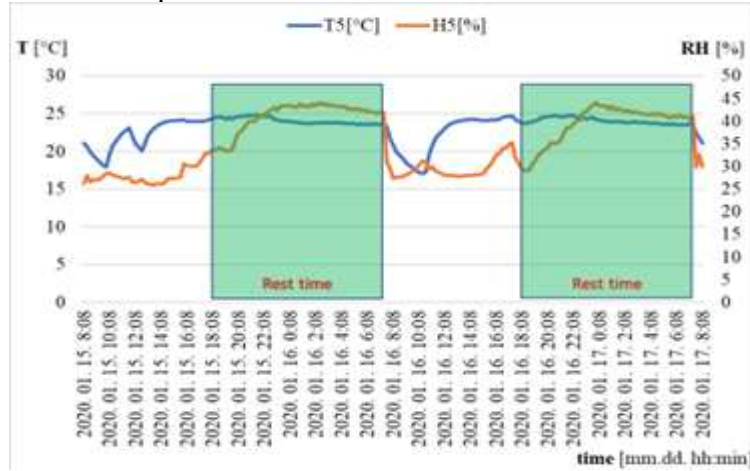

Figure 6. Hercegszántó HVB, 5. számú pihenőkörlet napi használata

The above intervals within a day can be properly characterized if I divide the 24-hour daily interval into 4 equal parts of 6 - 6 hours:
1) 00:00 – 06:00 - Rest time,
2) 06:00 – 12:00 – Duty time,
3) 12:00 – 18:00 – Duty time,
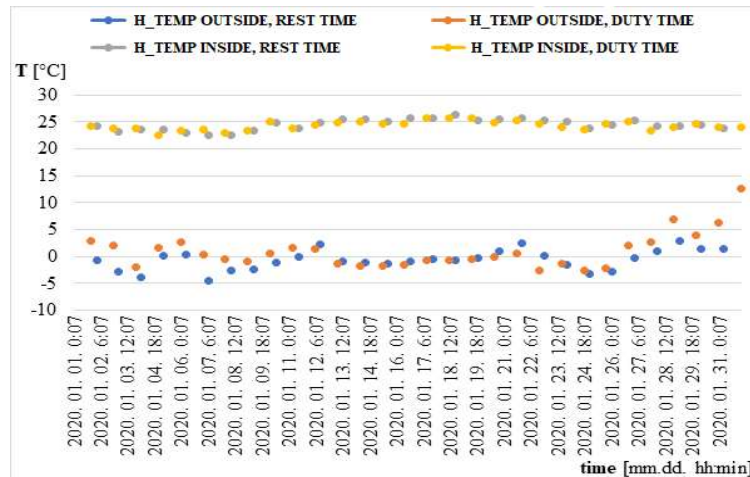4) 18:00 – 24:00 – Rest time.

Figure 7. Hercegszántó, 2020. januárban rögzített átlag hőmérsékleti adatok

26

According to the above distribution, for the month in January 2020, the average of the internal temperature readings, averaged over all 6 measuring units recorded at the same time, gave the following average temperature readings, plotted against the external temperature (Figure 9).

When the soldiers were in the resting area, they adjusted the internal temperature to their own subjective perception of temperature. The data collectors recorded an average internal temperature of 24.5 °C. During on-duty time, when the soldiers left the enclosure alone, although a certain energy-conscious behaviour of the soldiers in enclosure 5 was observed in Figure 9 (they turned down the heating when they left the enclosure), this was not generally the case, so data collectors recorded an average internal temperature of 24.3 °C in the resting enclosure during on-duty time, even in the month of January 2020. The average outside temperature during the rest period was -0.6 °C, while during the duty period the data collectors recorded an average of 0.9 °C, one and a half °C higher.

For a general characterisation of the value, I not only looked at the coldest period, but also at the beginning and end of the heating season. From the average calculation of the measured results, I have already shown that during the whole heating season, the average temperature set by the soldiers during their stay in the barracks was 24.5°C. If, by examining smaller intervals, I can show that the recorded average value of 24.5 °C is permanent, I consider the average of the measured values to be generally acceptable. Therefore, I have also compared the measured values with the sample taken at the beginning of the heating season with the sample taken at the end of the heating season. The result shows that the soldiers' subjective perception of heat in the quarters during this period averaged 24.4°C (Table 4).

Table 4, Temperatures at the beginning and end of the heating season

	first week of November		last week of March		Average values	
	Rest time	Duty time	Rest time	Duty time	Rest time	Duty time
1. day	24.1	23.9	23.7	24.1	23.9	24.0
2. day	25.1	25.1	24.0	23.6	24.5	24.3
3. day	25.8	25.7	23.2	24.3	24.5	25.0
4. day	25.9	26.2	23.7	24.0	24.8	25.1
5. day	25.1	25.0	24.0	23.5	24.5	24.2
6. day	24.8	24.8	23.7	23.6	24.2	24.2
7. day	24.7	24.5	23.5	22.3	24.1	23.4
	Average of measured values:				**24.4**	**24.3**

According to the data in Table 4, by symmetrically distributing the heating period and sampling the average values of the subjectively set temperatures, the average indoor temperature in the compartments during the rest period was 24.4 °C.

In this chapter, I have shown that, based on my measurements in real camp conditions, the average internal temperature set for the soldiers' subjective perception of heat in the camp rest quarters was 24.5 °C. The data were analysed for a total of one company (90 - 120 personnel) over several complete heating periods. By examining the measured data over several periods - at the beginning of the heating period, in the middle of the heating period and at the end of the heating period - I conclude that the individual-set internal temperature of 24.5 ± 1 °C was permanently present in the camp rest containers constructed from ISO 20' containers.

3.2 MLR model of the camp accommodation inside environment

The MLR model was tested between April 16, 2021 and June 19, 2021, with a total of 45 days of inputs (due to minor technical breaks), which of course include 6 days of identification and 39 days of validation.

3.2.1 *Identification and validation of the MLR model*

For the MLR model identification, 6 measured days were selected to represent a wide range of operating conditions over the two-month period under study. I also used these dates to identify the physics-based mathematical model, which are: May 4, 2021 (relatively windy day with high and uninterrupted/even sunshine intensity and high ambient temperatures), May 5, 2021 (a windy day with high but variable solar intensity and high ambient temperatures), 7 May 2021 (windy day with low solar intensity and low ambient temperature), 23 May 2021 (non-windy day with low sunshine and low ambient temperature), June 1, 2021 (a non-windy day with high and disturbed sunshine and low ambient temperatures), 16 June 2021 (a non-windy day with high and uninterrupted sunshine and high ambient temperatures).

Parameters to be identified in the MLR-based model are $c_{I,A1}$, $c_{k,A1}$, $c_{v,A1}$, $c_{b,A1}$, $c_{I,B}$, $c_{k,B}$, $c_{v,B}$, $c_{b,B}$, $c_{I,A2}$, $c_{k,A2}$, $c_{v,A2}$, $c_{b,A2}$ according to equations (34)-(36). To identify these parameters, I applied three standard independent MLR routines to the three separate operational cases (A1, B and A2) based on the measured data. The standard MLR routine (using the least squares method) is not detailed here as it is well known and can be found in most statistical and/or spreadsheet programs (Excel, SPSS, etc.). The left side of

Figures 11 and 13 show the comparison of the modelled (MLR) and measured internal temperatures of the camp container, and the right side shows the one modelled with the physics-based mathematical model during the identification on two days with quite different conditions: 2021. 04 May 2021 (windy day with high and uninterrupted solar radiation and high ambient temperature), 23 May 2021 (non-windy day with low solar radiation and low ambient temperature). Figures 10 and 12 show the measured solar radiation, ambient temperature and wind speed.
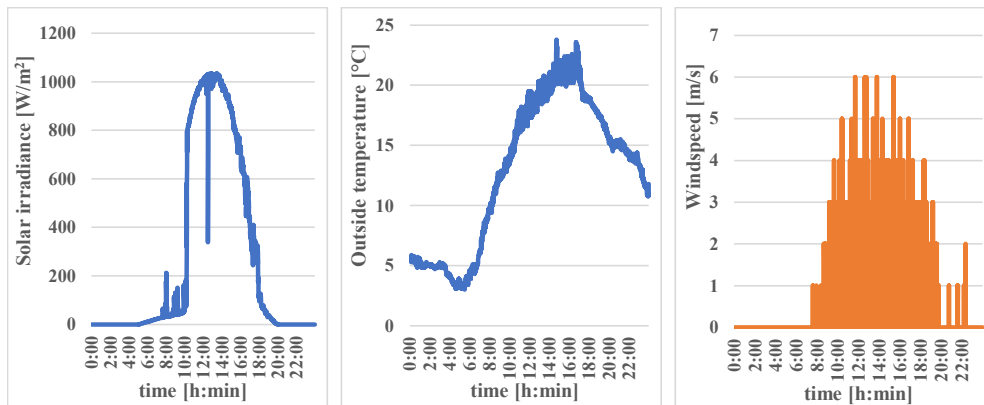

Figure 8. Measured environmental effects on 04.05.2021.
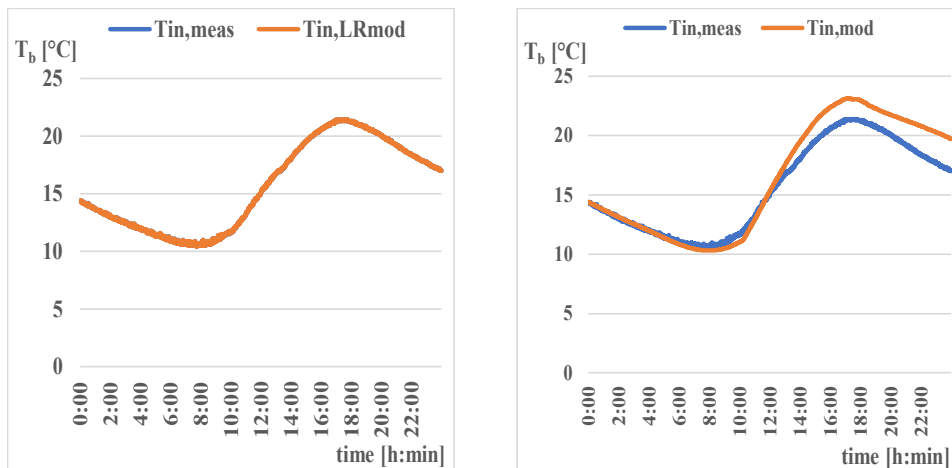

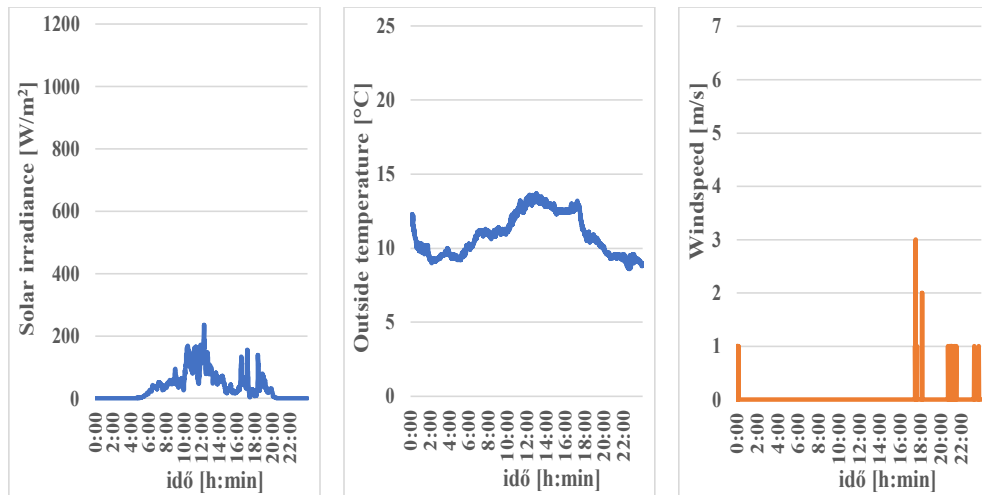Figure 9. Modelled and measured internal temperatures on 04.05.2021.

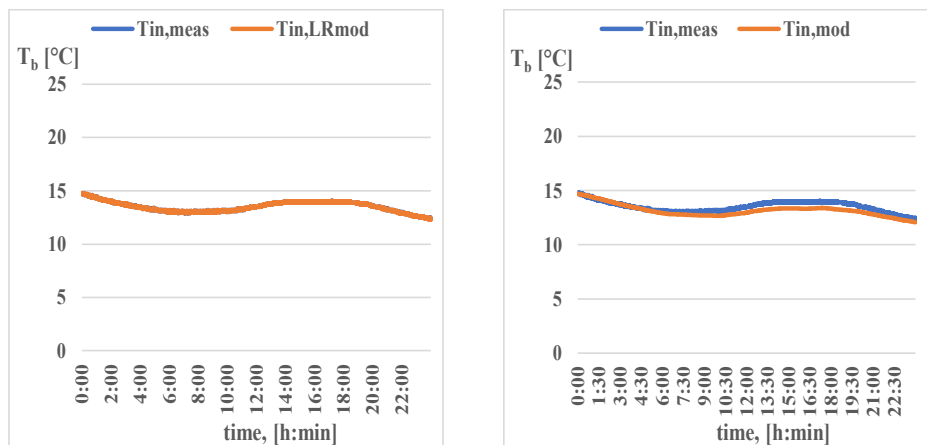Figure 10. Measured environmental effects on 23.05.2021.

Figure 11. Modelled and measured internal temperatures on 23.05.2021.

Table 5 summarizes the modeling deviations, as errors, which are the average value of the difference between the modeled and the measured internal temperature and the average of the absolute value of the modeling error.

The mean absolute error was calculated as the difference between the daily temperature range, maximum and minimum internal temperatures, in [%], using the error calculation method described in section 2.2.3 (3).

Table 5 shows not only the mean error and the mean absolute error for the two days of identification, but also the mean relative error for the whole 6

30

days of identification, which is $h_t = 0.7\%$ for the MLR model and $h_t = 12.0\%$ for the physical model.

Table 5: Average of error and absolute error values

		Physics-based model	MLR model
Identification	average error and absolute error mean values on 04.05.2021.	0.79 °C	-0.0005 °C
		0.99 °C; 9.0%	0.007 °C; 0.6%
	average error and absolute error mean values on 23.05.2021.	-0.35 °C	0.0007 °C
		0.38 °C; 15.0%	0.04 °C; 1.5%
	Mean relative error of identification (6 days)	**12.0%**	**0.7%**
Validation	average error and absolute error mean values on 17.05.2021	-0.28 °C	-0.23 °C
		0.54 °C; 22.6%	0.28 °C; 11.5%
	average error and absolute error mean values on 17.06.2021	-0.95 °C	0.49 °C
		0.95 °C; 8.1%	0.49 °C; 4.2%
	Mean relative error of validation (39 days)	14.8%	<u>**7.1%**</u>

Validation

For the validation of the MLR model, I used the already identified physics-based and MLR-based models with inputs for a total of 39 days (due to minor technical breaks) measured between 16 April 2021 and 19 June 2021, which of course excludes the 6 days of identification. I compared the modelled internal temperature with the measured temperature and evaluated the difference, i.e. the error, for both models.

Figures 15 and 17 show the modelled and measured internal temperatures for both models on the two days of validation, a windy day with low solar radiation and low ambient temperature on 17 May 2021 and a non-windy day with high and disturbed solar radiation and high ambient temperature on 17 June 2021. Figures 14 and 16 show the measured solar radiation, outdoor temperature and wind speed on the same two days.
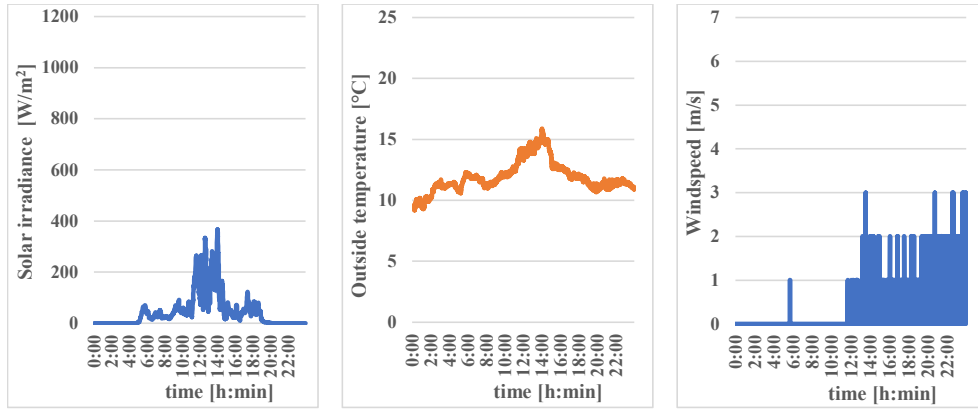
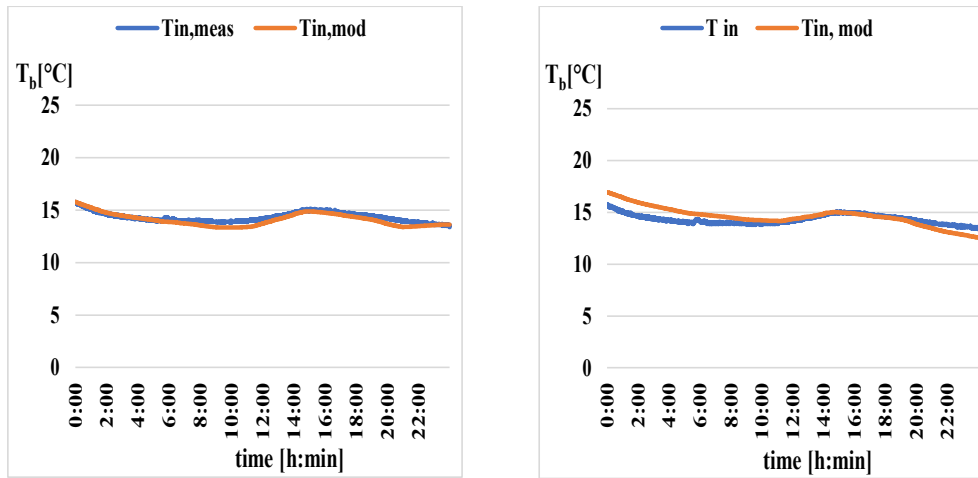Figure 12. Measured environmental effects on 17. 05. 2021.

Figure 13. Modelled and measured internal temperatures on 17. 05. 2021.
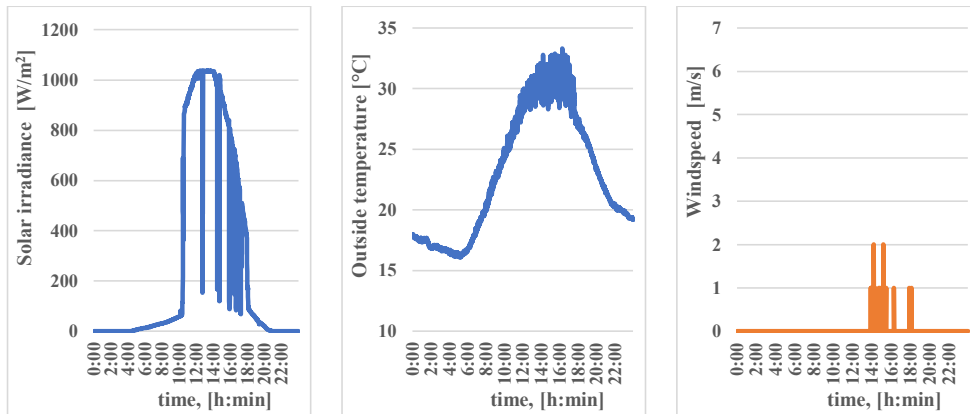

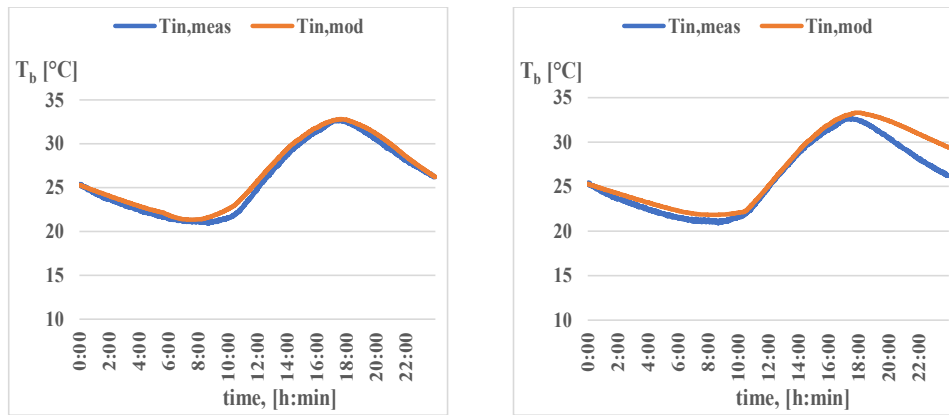Figure 14. Measured environmental effects on 17. 06. 2021.

Figure 15. Modelled and measured internal temperatures on 17. 06. 2021.

The validation results are also summarized in Table 5, which shows that the internal temperature of a container manufactured according to the ISO standard, also used for the deployment of military camps, can be described quite accurately by an MLR-based model, in this case more accurately than the widely used physics-based model. The validation shows a modelling error of $h_t = 7.1\%$ for the MLR-based model, compared to $h_t = 14.8\%$ for the physics-based model. The accuracy of the MLR-based model is considered to be good for general engineering purposes such as studying and predicting the internal temperature variation of ISO containers. Among other applications, this prediction can also be used to predict the heating/cooling capacity required for a comfortable temperature inside the container for a comfortable thermal environment.

3.2.2 Identification and validation of the M63 tent MLR model

The way in which military camps are built is primarily determined by the method and time of deployment. However, there is no sharp dividing line between the use of a container-built camp and a tent-built camp. As a missing piece of work, I also saw the need to obtain research results that would help to make the decision when to apply a stable construction material camp or a tent material camp to ensure the execution of a planned operation. For this reason, I also collected data on the internal temperature of the M63 sample tent.

For the tent model identification, I selected the same 6 measured days as for the container study, so that the operating conditions represented the same range over the two-month period studied, with solar radiation and wind speed values shown in Figures 18 and 19.
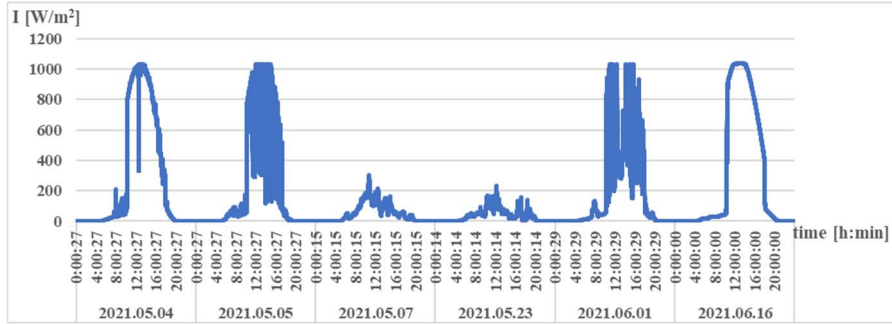
Figure 16. Global radiation values for days selected for identification
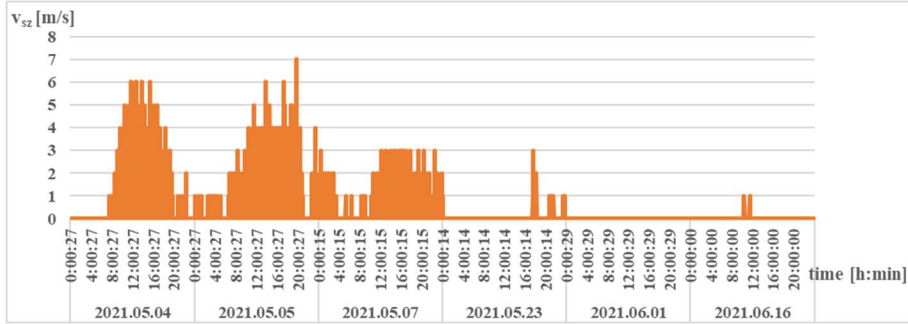
Figure 17. Wind speed values for days selected for identification

The measurements clearly show the difference in the physical properties of the two materials, which makes the internal temperature of the tent more sensitive to external environmental influences. This difference is illustrated in Figure 20 on 05 May 2021, selected for identification, and 14 June 2021, selected for validation.
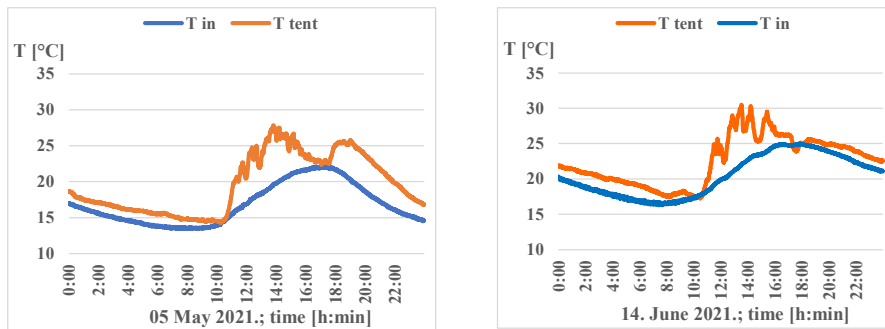
Figure 18. Container and tent internal temperature

The parameters are also the same for the MLR-based model identification $c_{I,A1}$, $c_{k,A1}$, $c_{v,A1}$, $c_{b,A1}$, $c_{I,B}$, $c_{k,B}$, $c_{v,B}$, $c_{b,B}$, $c_{I,A2}$, $c_{k,A2}$, $c_{v,A2}$, $c_{b,A2}$, as for the container according to equations (5)-(7). Identification of these parameters

34

was also performed using three standard independent MLR routines based on the measured data from three separate operational cases (cases A1, B, A2).
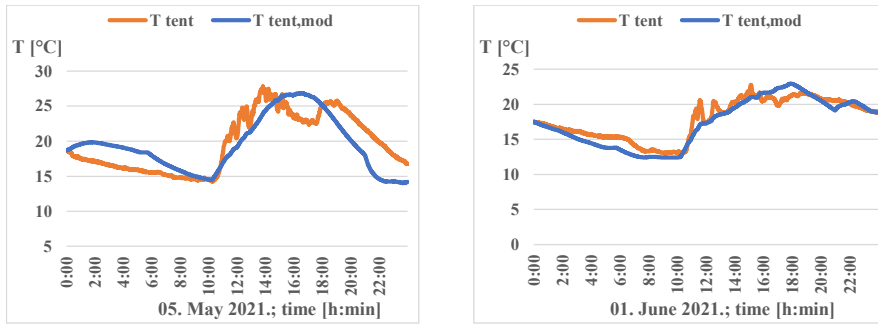
Figure 19. Tent measured and modeled temperatures during identification.

Figure 21 shows a comparison of the modelled and measured internal temperatures of the M63 tent on two different days of identification. Both days were characterised by high-intensity but scattered sunshine, but it was windy on 5 May 2021 and windless on 01 June 2021.

Table 6 shows the mean of the error as the average of the difference between the modelled and measured internal temperature, and the mean of the absolute error for the above two days of identification, which is the average of the difference between the modelled and measured internal temperature, also corresponding to the absolute error calculation method (3) presented earlier in Section 2.2.3, expressed as [%] proportional to the difference between the maximum and minimum daily measured internal temperature.

Table 6, Average of the M63 tent temperature MLR model error values

Error and absolute error mean values		M63 MLR model
Identification	05 May 2021.	-0.15 °C
		2.41 °C; 17.7%
	01. June 2021.	-0.47 °C
		0.87 °C; 8.9%
	Identification error average % (6 days)	10.2%
Validation	17 May 2021.	-0.07 °C
		1.07 °C; 10.7%
	14 June 2021.	-0.58 °C
		1.45 °C; 11.0%
	Validation error average % (39 days)	**_7.8%_**

35

Table 6 presents not only the mean and the absolute mean error for the two days of identification, as shown for the container model. The average of the error values for all 6 days of identification is presented with basically worse values (h_t = 10.2%) than for the camping container model, but it is still useful for comparing the two camping specialties.

Validation

For the validation of the internal temperature MLR model of the M63 tent, I used the already identified model, also with a total of 39 days of inputs between 16 April 2021 and 19 June 2021, which of course does not include the 6 days of identification.

The modelled internal temperature was compared with the measured temperature and the difference between the two values, i.e. the error, was evaluated. Figure 22 shows the modelled and measured internal temperatures on two days of validation under quite different operating conditions; a windy day with low solar radiation and low ambient temperature on 17 May 2021 and a non-windy day with high and disturbed solar radiation and high ambient temperature on 14 June 2021.
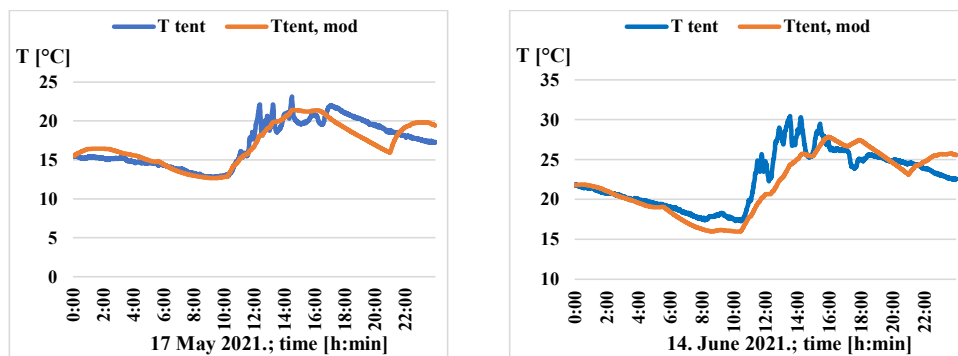
Figure 20. Modelled and measured temperatures during validation

Based on the results, I conclude that the internal temperature of the M63 sample tent can be described fairly accurately by the MLR-based model. The validation shows that the modelling error of the MLR-based model is h_t = 7.8%. Although there is still room for further refinement of the accuracy of the MLR-based model of the tent material, it is already adequate for the general engineering and military purposes of studying and predicting the internal temperature variation. This prediction can be used, among other applications, primarily to determine the application time period of tent and

container materials, and secondarily to calculate and plan the heating/cooling capacity required to maintain a comfortable temperature level inside the tent.

3.2.3 Container IAQ - CO₂ concentration MLR model validation

For the MLR model identification of camping containers, 2+4 measured days were selected to cover a wide range of possible operating conditions. First, I selected a measured day with a large indoor-outdoor temperature difference coupled with high winds and steady indoor concentrations (05 April 2021). Next, I selected a day where the outside-inside temperature difference is not large, but is coupled with a large wind with a monotonically increasing internal concentration (15 and 16 April 2021). Then I selected a day where a large outside-inside temperature difference is coupled with a small wind with a steady internal concentration (15 and 16 April 2021). 18 April 2021) and a day with a large outside-inside temperature difference coupled with low winds and a monotonically increasing internal concentration (15 and 16 June 2021). The 2+4 days proved to be sufficient to obtain a model with a reasonably good accuracy. For the sake of practice, these days were selected from the last third of spring and the first third of summer, so that the identified model can be used for the remaining months of spring, summer and autumn.

Figures 24 and 26 compare the modelled and measured internal concentrations. The figures show that the MLR model (K_bMLR_mod) values are almost identical to the values measured in the ISO container (K_b).
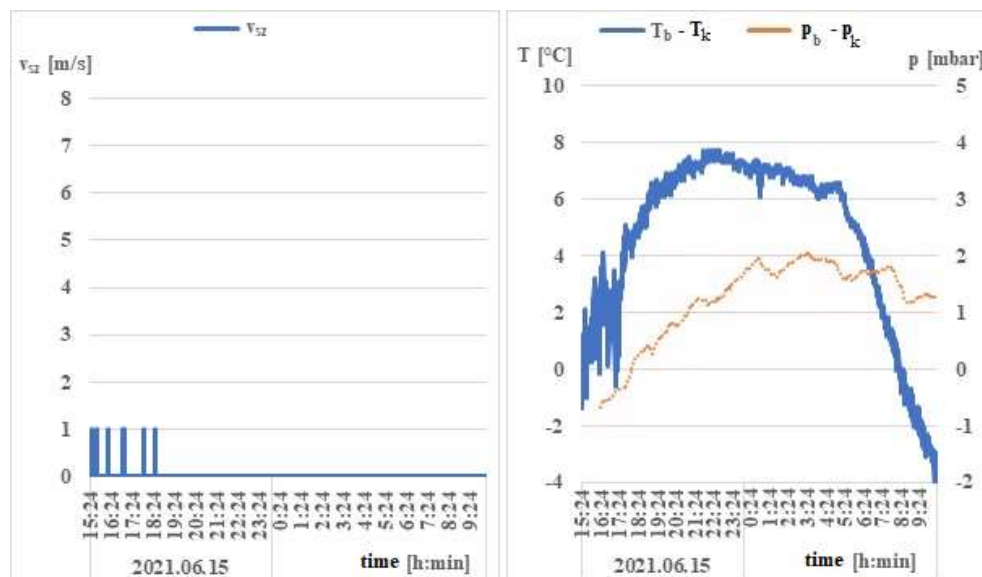
Figure 21. Measured environmental effects on 15-16. June. 2021.
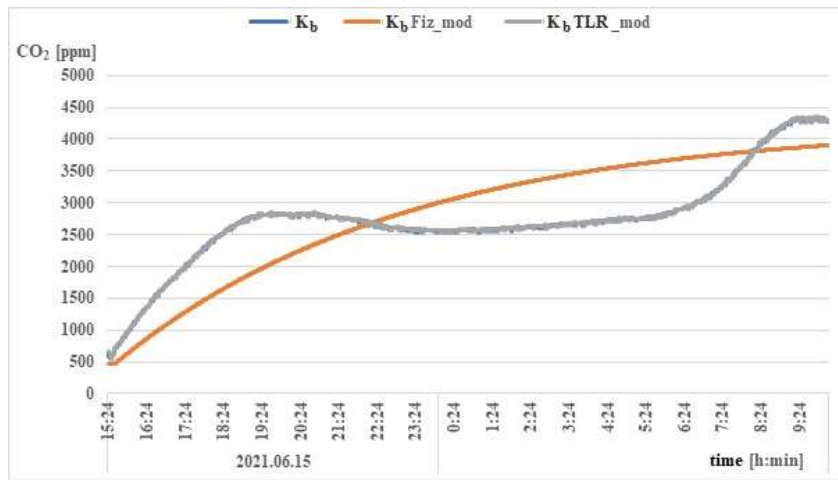
Figure 22. Modelled and measured concentration on 15-16. June 2021

Figures 23 and 25 show the wind speed, the difference between outside and inside temperature, and the difference between outside and inside atmospheric pressure on the same day. The figures clearly show that the difference between outside and inside temperature and the difference between outside and inside atmospheric pressure describe similar.
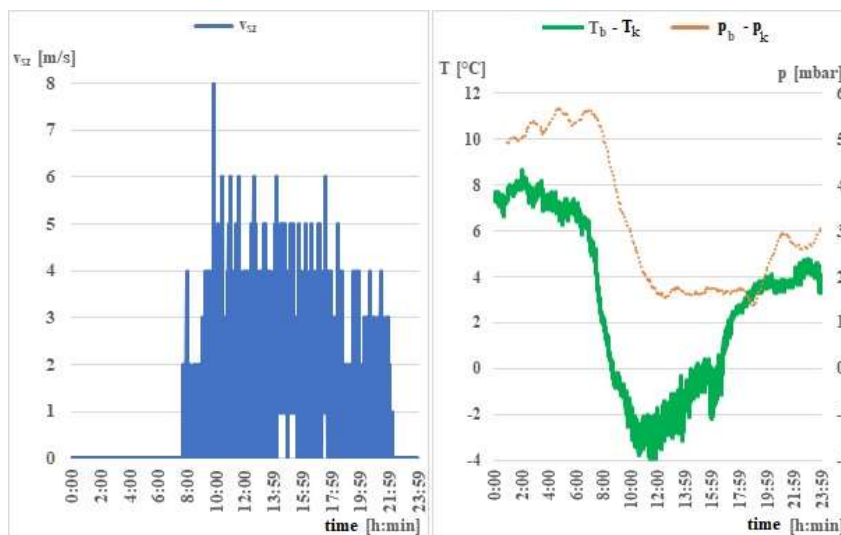
Figure 23. Measured environmental effects on 05. April. 2021.

Table 7 summarises the modeling discrepancies, as errors, which are the mean value of the difference between the modeled and measured internal carbon dioxide concentrations and the average of the absolute value of the modeling error.

38
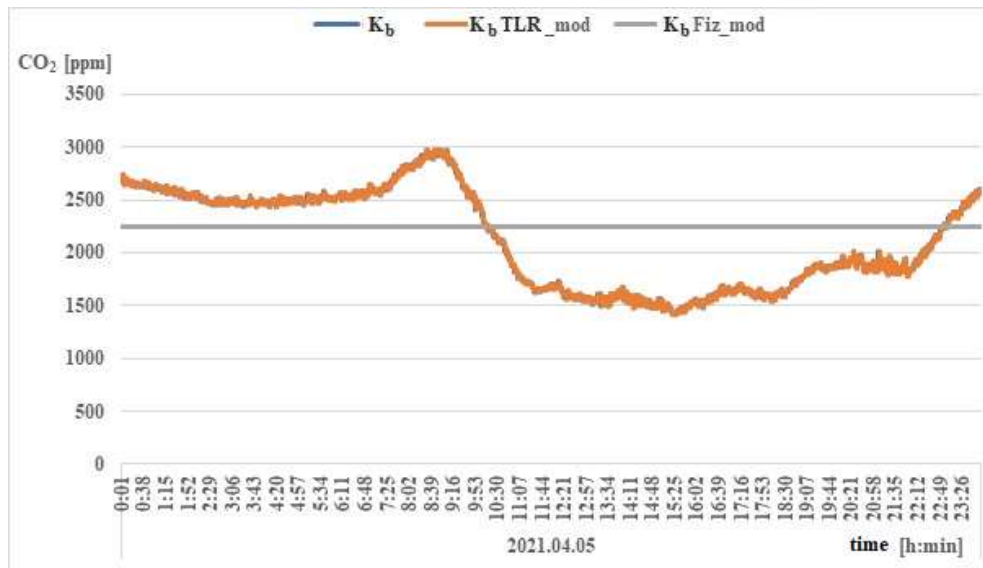
Figure 24. Modelled and measured concentration on 05. April. 2021.

The mean absolute error is expressed as the difference between the daily concentration interval, i.e. the maximum and minimum measured carbon dioxide concentration, in [%], according to the error calculation method described in section 2.2.3 (3).

Table 7, Absolute error values and % mean for the models

Measured absolute mean error and incidence rate		Physics-based model	MLR model
identification	05. April	429 ppm; 27 %	14,6 ppm; 0,9%
	15-16. June 2021.	500 ppm; 13 %	8,5 ppm; 0,2%
	Average error % of total identification (4+2 days)	11.0%	**0.3%**
Validation	08-09. April	652 ppm; 19.7 %	250 ppm; 7.7 %
	30. April – 01. May	421 ppm; 22.5 %	353 ppm; 18,8%
	Average error over the entire validated period of 31 days. (01. April – 26. June)	12.4 %	**9 %**

39

In the MLR-based model identification, I used a standard MLR routine to determine the parameters c_K, $c_{\Delta T}$, c_V, c_{Kb} and c., based on the measured data in equation (8). The standard MLR routine (based on the method of least squares) is well known and available in most statistical and spreadsheet programs (SPSS, Excel, etc.), so I will not detail it here. In our case, the indicators in Table 14 are more relevant and more expressive, especially for comparison with a physics-based model than for comparison with a model already accepted in the literature. Table 7 shows the mean and mean absolute error values for the 1+2 days presented in the results (April 5, 2021 and June 15-16, 2021). The mean of these % values for each of the 2+4 measurement days for the MLR model identification is also presented in Table 7 ($h_t = 0.3\%$). The mean error % value for the physical-based model for the entire 2+4 days of identification is also presented in Table 7 ($h_t = 11.0\%$).

For validation, I apply the already identified physics-based and MLR-based models with the following corresponding inputs measured over the remaining period. Specifically, I change one of the inputs of the MLR-based model relative to the inputs of the identification, namely the modeled value $K_{b,mod}(t-\tau 2)$ and the value $K_b(t-\tau 2)$ in the MLR-based model (8) (rather than $K_{b,meas}(t-\tau 2)$).

The modelled days are between 1 April 2021 and 26 June 2021, which gives a total of 31 measured days for validation due to minor technical interruptions in operations. The modelled and measured output carbon dioxide concentrations were compared and evaluated for both models. Table 7 shows the average error and the mean of the absolute error values for the two validation days presented in this thesis. The calculation of the mean of the absolute error values is the same as the calculation of the error value (in %) used for the identification. These % values are also shown in Table 7 for the whole modelled period from 01 April 2021 to 26 June 2021. $h_t = 12.4\%$ for the physics-based model and $h_t = 9\%$ for the MLR-based model.

Figures 27 and 29 show the wind pressure/wind speed acting on the total container surface and the difference between the ambient temperature and the internal temperature with internal and external atmospheric pressure measured on the same days.

40
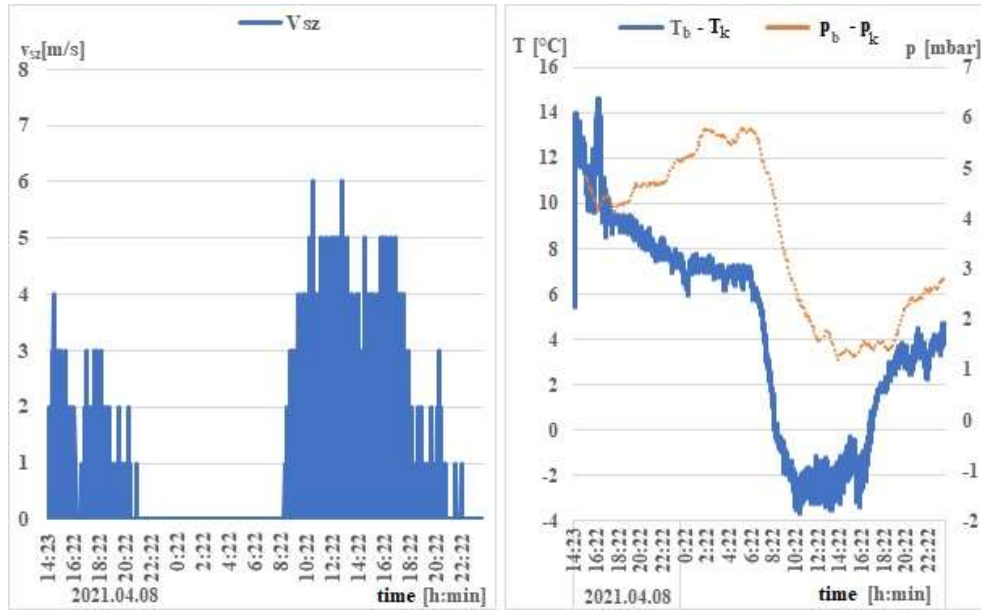
Figure 25. Measured environmental effects on 08-09 April 2021.

Figures 28 and 30 show the modelled and measured output concentrations for the two models for a monotonically increasing concentration due to the appearance of a point source (08-09 April 2021) and a theoretically adjusted concentration due to the internal point source on a windy day (30 April - 01 May 2021).
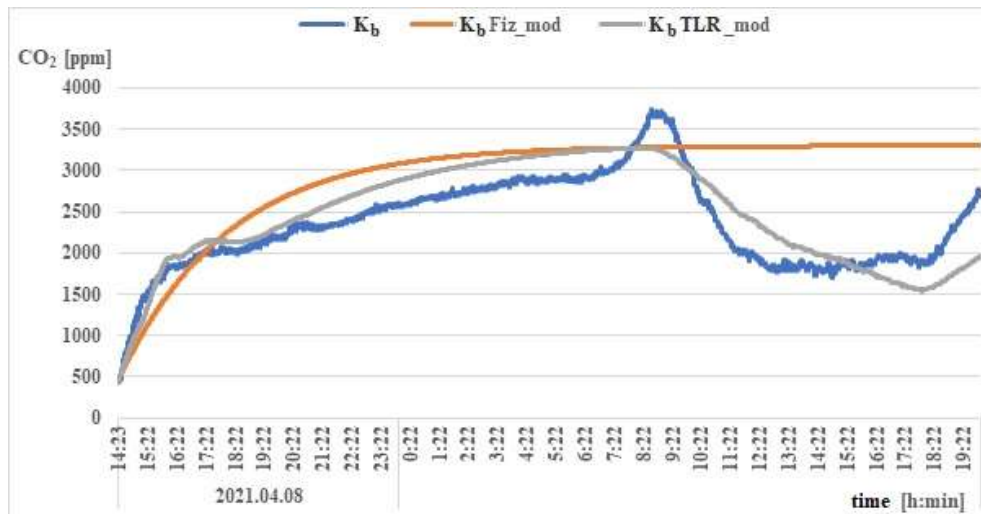
Figure 26. Modelled and measured concentration on 08-09 April 2021.
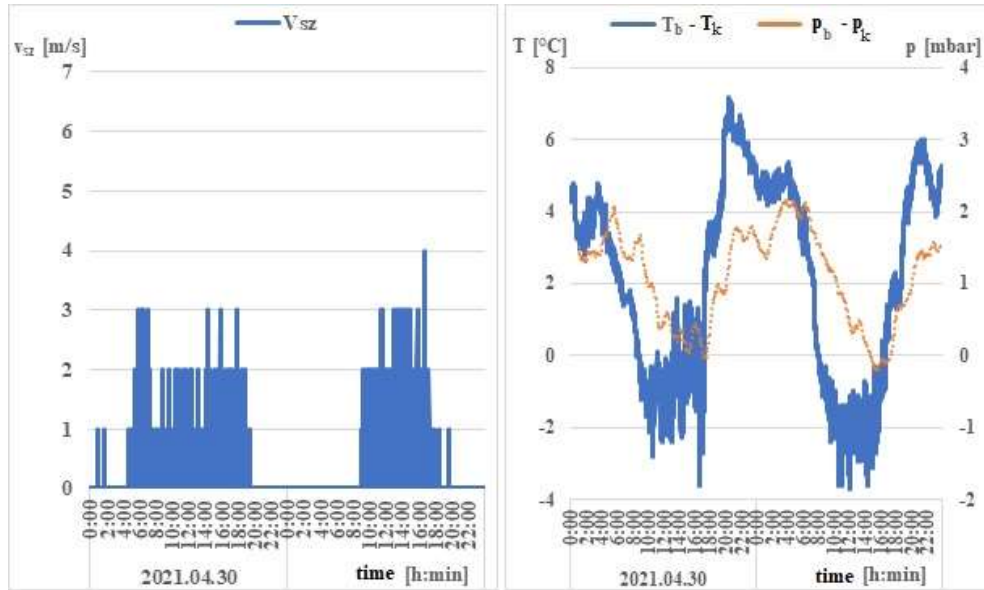
Figure 27. Measured environmental effects on 30 April – 01 May 2021.
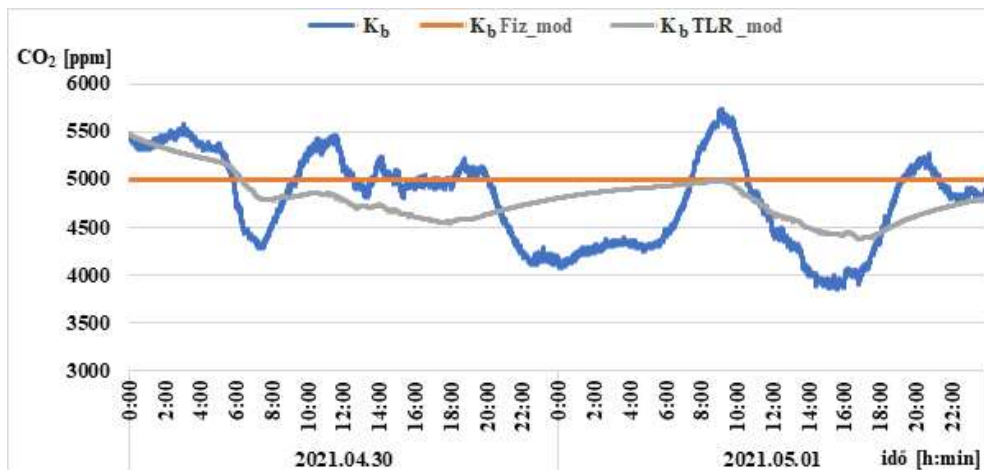
Figure 28. Modelled and measured concentration 30 April – 01 May 2021.

I conclude that the indoor air quality concentration in the camp accommodation container can be modelled well with the MLR-based model and more accurately than with the physics-based model. Based on the validation, the average modelling bias as error is below 10% (h_t = 9%) with the MLR-based model, which error is h_t = 12.4% for the physical model. Note that the accuracy of the physics-based model is also reasonable and in line with values presented in previous literature, where the filtration of the container was constant.

42

3.3 Effect of elevated CO₂ in indoor air on military capability

In the experimental situational shooting, the results recorded as a measure of military skill performance were assessed by measuring the hit point score [KP] of 5 shots, the mean distance from the centre hit point [SD] and the time taken to complete [t].

Based on the results presented, it can be assumed, as the graph showing the average results (Figure 31) clearly illustrates, that the efficiency of the situational shooting skill performed in the experiment is reduced when the task is performed for at least 70 minutes from an indoor environment with CO_2.
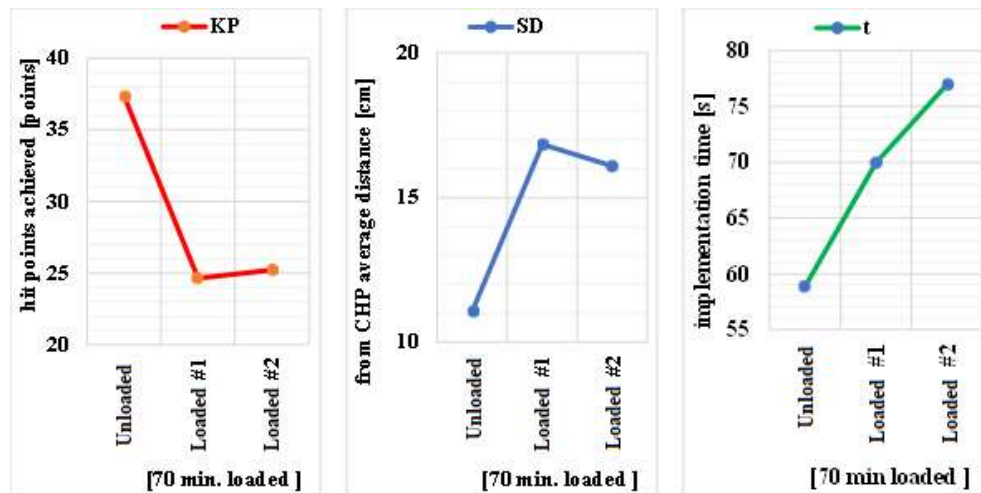
Figure 29. Average results of shooting

The graph clearly shows that the hit rate decreases, the impact dispersion of the projectiles increases and the execution time also shows a marked increase, so the soldier's concentration, accuracy and speed decrease, thus lowering his combat performance. In the following, the effectiveness of some indicators is presented separately.

3.3.1 KP- hit score

Using the method described in section 2.3.3 (11), the change in the efficiency of the hit score and the change in the efficiency of situational shooting initiated from a CO_2-loaded indoor environment, as a proportion of the results obtained from an unloaded environment, can be shown for each of the 3 series of participants for the results of the first load shooting and the second load shooting, which are shown in Figure 32.

43
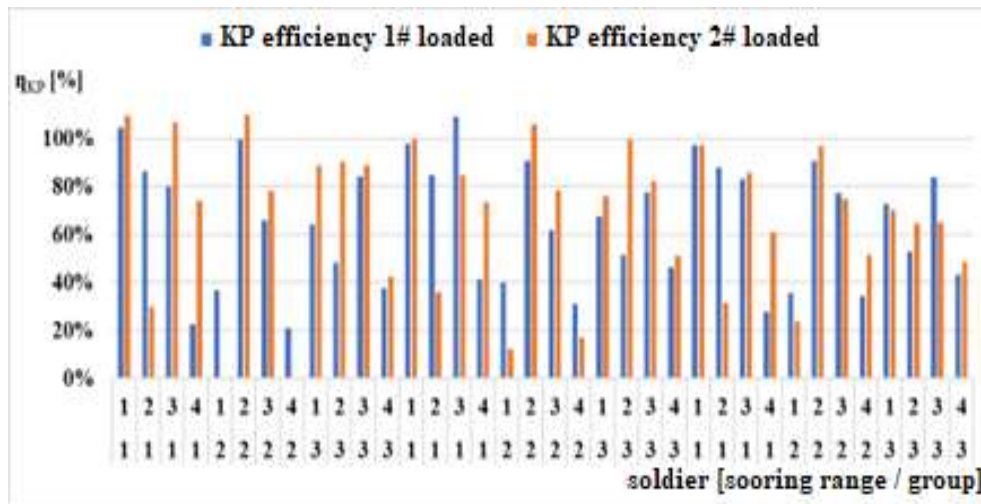
Figure 30. KP efficiency for each soldier

To compare the results of shooting after 70 min of unloaded and 70 min of loading at carbon dioxide concentrations above 3000 ppm, shown in Figure 32, I performed two-sample t-tests (16) and checked the significance level of the difference detected.

First, I compared the hit point (KP) values of the unloaded and the 70 min loaded shots. One group performed situational shooting in 4 firing positions in 3 shifts, so 12 soldiers averaged 5 shots hit score, 12 - 12 to be evaluated as KP, the number of shots fired both unloaded and after 70 min of exposure to air with carbon dioxide concentration above 3000 ppm. The resulting hit score for 't' in the student table is: **$t_{KP}=3,257$**

Table 8, critical limits for t-test significance level
Student or t distribution

	'P' value =	0,9995	0,995	0,99
	α =	0,001	0,01	0,02
	significance level =	99,9%	99,0%	98,0%
$t_\alpha = \Phi^{-1}_{n+m-2}\left(1-\frac{\alpha}{2}\right) =$		**3,792**	**2,819**	**2,508**

Considering the t-value for the hit score outside the critical range shown in Table 8, **2.819 < t_{KP} < 3.792**, the difference in hit score (KP) between unloaded and 70 min post-loaded shots is significant at a significance level of **$p \leq 0.005$**.

I also performed a t-test to check the significance level of the difference in the shooting results after the first and second 70 min of loading. The value obtained is t = - 0,402, which indicates that the significance level of the difference between the two results is only 40 %, so that no firm conclusion can be drawn from the results.

Based on the evaluation of the KP results of loaded and unloaded situational shooting, averaged as a parameter of military capability, the average of the effectiveness over the whole population is presented in Table 9, which shows that the accuracy of the hits dropped to 2/3 after the first 70 minutes of confined space above 3000 ppm carbon dioxide concentration.

Table 9, Results of loaded and unloaded situational shooting (KP)

sn	CO_2 load above 3000 ppm	KP result change
1	0 min. – i.e. unloaded	100%
2	1 x 70 min. after load	65%
3	2 x 70 min. after load	67,5%

3.3.2   SD- Average distance from the centre hit point

Using the method presented in section 2.3.3 (12), the average distance from the mean hit point, i.e. the efficiency evaluated from the standard deviation, and the change in efficiency of situational shooting initiated from a CO_2-loaded indoor environment at a rate similar to that of shooting from an unloaded environment, as for the hit score.

Figure 31. SD efficiency for each soldier

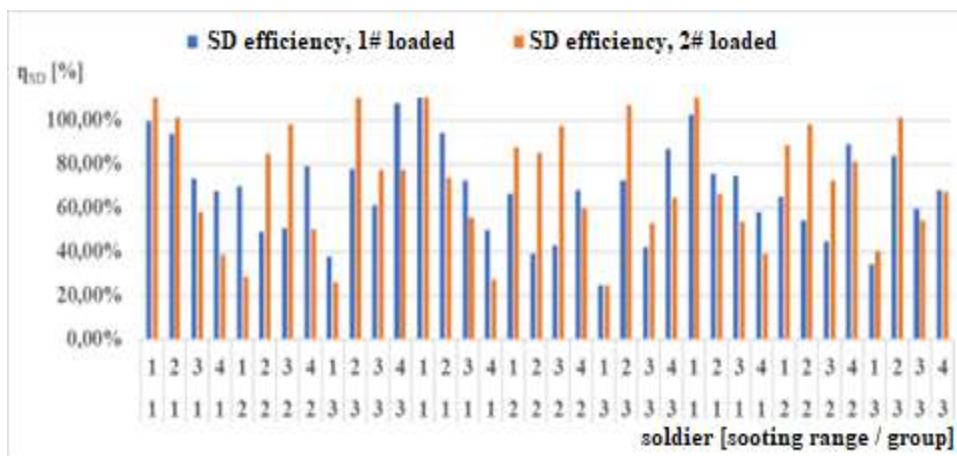For each of the 3 series, the results of the first load shooting and the second load shooting were detected for each fighter (Figure 33). To compare the

45

results of the unloaded - and after 70 min of loading at carbon dioxide concentrations above 3000 ppm, shown in Figure 33, I performed two-sample t-tests (16) and checked the level of significance of the difference detected. According to the student's table, considering the values presented in Table 9, the t - value of the standard deviation outside the critical range, **-2.819> t_{SD} >-2.508**, confirms that the difference in SD results between unloaded and after 70 min of loading shooting is significant at a significance level of **p ≤ 0.01**. Student's t' for the standard deviation is **t_{SD}= - 2.591**.

I also performed a t-test to check the level of significance of the variance of the first and second 70 min post-loading shots. The value obtained is t = - 0.553, which indicates that the significance level of the difference between the two standard deviations is only 50 %, so that no firm conclusion can be drawn from the difference in the results.

Based on the assessment of the SD score of loaded and unloaded situational shooting, averaged as a parameter of military capability in a similar way as I did for the hit score, I have shown the averaged value of effectiveness over the total force in Table 10. I find that the standard deviation has dropped to more than 3/4 of the standard deviation after only the first 70 minutes in a confined space above 3000 ppm carbon dioxide concentration.

Table 10, Results of loaded and unloaded situational shooting (KP)

sn	CO_2 load above 3000 ppm	SD result change
1	0 min. – i.e. unloaded	100%
2	1 x 70 min. after load	70%
3	2 x 70 min. after load	76%

3.3.3   t - implementation time

Using the method described in Section 2.3.3 (13), the change in execution time efficiency and the change in situational firing efficiency initiated from a CO_2-loaded indoor environment as a proportion of the execution time from an unloaded environment can be shown for each of the 3 series of executors for the results of the first loaded firing and the second loaded firing (Figure 34).

To compare the results of shooting after 70 minutes of unloaded - and after 70 minutes of loading at carbon dioxide concentrations above 3000 ppm, shown in Figure 34, I performed two-sample t-tests (16) and checked the significance level of the difference detected.

Figure 32. (t) efficiency for each soldier

The t-value (t_t = - 3.245) of the execution time outside the critical range (as shown in Table 9), - 2.819 > t_t > - 3.792, confirms that the difference in the execution time result (t) between the unloaded and the 70 min post-load shooting is significant at a significance level of p ≤ 0.005.

I also performed a t-test to check the significance level of the execution time of the first and second 70 min post-loading shootings. The obtained value is t = - 2.105, which indicates that the difference in the (t) time result between the 70 min and 2x70 min post-load shooting results is significant at a significance level of p ≤ 0.025.

Based on the evaluation of the results of the situational shooting execution time (t), I have shown (in Table 11) that the time required to solve the situational shooting increased on average by 1/5 of the first 70 min and 1/3 of the second 70 min after the first 70 min of confined space above 3000 ppm carbon dioxide concentration.

Table 11, Results of loaded and unloaded situational shooting (t)

sn	CO_2 load above 3000 ppm	t result change
1	0 min. – i.e. unloaded	100%
2	1 x 70 min. after load	80%
3	2 x 70 min. after load	67%

3.3.4 Efficiency indicator

Using the calculation method (17) presented in the Materials and Methods chapter, the change in the effectiveness of situational shooting initiated from a CO_2-loaded indoor environment can be shown for each of the 3

47

experimental series for each fighter for both the first load shooting and the second load shooting results (Figure 35).
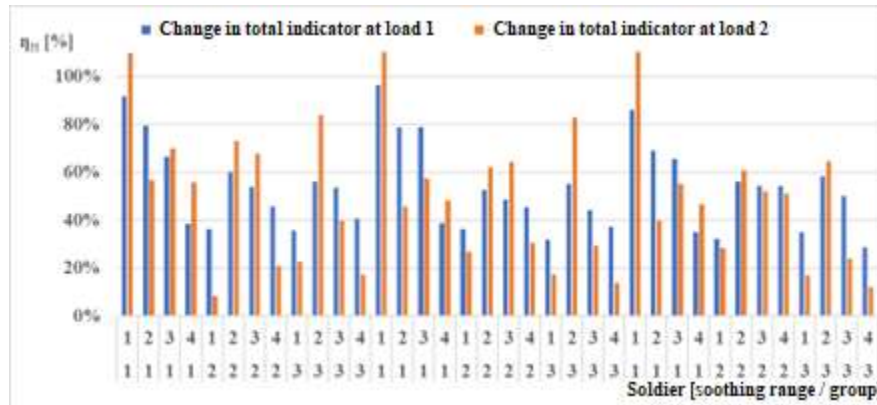
Figure 33. Change in combat capability effectiveness

Based on the results of the situational shooting, I evaluated the combat capability index, averaged the effectiveness results (17) and showed (Table 12) that the soldiers' shooting capability to solve the defined situation was halved after the first 70 minutes of confined space above 3000 ppm carbon dioxide concentration. After the second 70 minutes in a confined space above 3000 ppm carbon dioxide, the decrease in effectiveness further increased.

Table 12, Performance of loaded and unloaded situational shooting (ηH).

sn	CO_2 load above 3000 ppm	η_H result change
1	0 min. – i.e. unloaded	100%
2	1 x 70 min. after load	54%
3	2 x 70 min. after load	49%

I tested the effects of carbon dioxide concentration on soldiers by performing situational shooting. I found that, consistent with similar research, above 3000 ppm concentration, soldiers' performance deteriorates significantly. However, a new finding is that, unlike office workers, the large degradation effect on military capability does not occur after 3x70 minutes, but after the first 70 minutes of exposure.

After 70 min of loading, the efficiency of the military capability was reduced by almost half based on the evaluation presented. After 2 x 70 min of loading, the performance decrease was no longer pronounced. Evaluated as a function of the results after the first load, the efficiency of task performance after the second load was only 10% worse.

48

4   CONCLUSIONS AND RECOMMENDATIONS

There is no doubt that it is important to develop more practical and/or accurate mathematical models to describe indoor temperatures or pollutant concentrations in order to determine the indoor air quality of buildings, as this is the most important variable in the indoor environment of buildings that determines human comfort. In my thesis, I evaluated the subjective thermal sensation of individual soldiers and the effect of elevated carbon dioxide concentrations, and developed a new, easy-to-use, black-box model with low computational requirements for determining the indoor temperature of ISO 20' containers used for human occupancy and the expected development of carbon dioxide concentrations..

4.1   Thermal comfort measurement

The internal temperature requirements associated with subjective thermal comfort are set out in standards, and as I have shown in the literature review, the so-called comfortable thermal comfort is the state of mind that expresses satisfaction with the thermal environment. If, for a given activity, an individual can dissipate heat to the environment in such a way that a core temperature of 36 - 37 °C is achieved and the skin temperature remains at an appropriate level, then the individual considers his/her environment to be thermally comfortable. Thermal calculations and heat balance calculations can be performed for several conditions under consideration. Previous research has investigated individual thermal comfort, and later a nonlinear autoregressive network model was developed to predict indoor temperature. According to the current standard, the design basis values for buildings and spaces for different purposes, for residential and office buildings, are set at 22 ± 1 °C indoor temperature as the winter design basis value.

The heating of the camp facilities is provided by an ISO 20' container equipped with an electric convection heater, so the required internal temperature is sized for the internal air temperature in the case of convection heaters. Therefore, the aim of my research is to measure the average value of the air temperature set for the subjective thermal sensation of the soldier as an individual in the resting enclosure of the ISO 20' container, during heating.

Based on my measurements in real camp conditions, the average internal temperature in the camp's rest areas, set to the soldiers' subjective thermal sensation, was 24.5°C. The data were measured for a total of one company

(90-120 personnel) over several complete heating periods. By examining the measured data over several periods - at the beginning of the heating period, during the coldest month of the heating period and at the end of the heating period - I conclude that the average set internal temperature of 24.5 °C was permanently present in the rest containers.

A control calculation of the heating heat demand of the 160-strong border protection base(s) deployed on the southern border was carried out at the time of the takeover (2017), according to which the heating power was defined as 911 W heating heat demand per container. The current standards do not differentiate between temporary installations, therefore the heating temperature sizing was performed for a minimum temperature of 22 ± 1 °C, taking into account the design basis available for the built environment, which resulted in an external transmission heat loss of 24.5 kW and a filtration heat loss of 25.8 kW for the whole installation.

In the light of the air temperature value set for the subjective thermal sensation presented in my thesis, I recognized the fact that my previous design calculation was flawed. Recalculated according to an internal temperature design data of 24.5 °C, the external transmission heat loss is 27 kW and the filtration heat loss of the installation is 29.7 kW. Thus, the installation of a device with a heating thermal capacity of 1031 W in the containers is required.

With the recent significant changes in the energy market, more accurate energy demand calculations have been a priority. The two calculated heat output results differ by 13.2 %, which is already a relevant discrepancy in engineering practice, and therefore in general engineering practice I consider it of high importance that the design baseline data for different installations are continuously monitored and refined.

4.2 Inside temperature modelling of a Military Camp facility

In contrast to building energy modelling presented in the literature, the MLR-based model proposed in my study predicts the indoor temperature at a given modelled time as a function of the ambient temperature, as well as solar radiation and wind speed - and the modelled indoor temperature corresponding to the previous time as a certain initial condition. The model predicts the output in time detail, i.e. every half minute (not just every day or several hours).

Based on the results showing the internal temperature modelling of the ISO 20' container as a camp unit building, I conclude that the internal

temperature of the ISO 20' container can be accurately described by the MLR-based model, and much more accurately than the widely used physics-based model. The validation shows that the MLR-based model has a modeling error of 7.1% and the physics-based model has a modeling error of 14.8%. Therefore, the accuracy of the MLR-based model is considered to be very good for general engineering purposes, i.e. it is suitable for studying and predicting indoor temperature changes in military camp housing containers. This prediction, among other applications, can serve as an approximate estimate of the heating/cooling capacity required to maintain a comfortable temperature inside the container.

For the validation, I also determined the correlation coefficient R^2, which describes the difference between the modelled and measured results, which is 0.9738 for the validation of the physics-based model and 0.9885 for the validation of the MLR-based model. These values confirm that the MLR-based model has higher accuracy than the physics-based model.

The (relative) modelling error of the MLR-based model is 7.1% over the entire validation period. Since the maximum recorded difference between the daily maximum and minimum measured indoor temperature is 13.5 °C during the validation period (9 May 2021), this implies an absolute error of up to 13.5 * 0.07 = 0.9 °C (average) for any given day. The average value (for all days of the validation) is much better, around 0.5 °C. This is an acceptable accuracy for general engineering purposes such as (pre-)predicting or maintaining a calculated indoor temperature, since a thermostat controlling a heating system operates in a similar range.

Due to the simple linear, explicit relationships for indoor temperature, the MLR-based model has very low equipment/device requirements. Accordingly, only the most basic computing tools are required (e.g. Excel or similar software), which is a great advantage in practice.

The MLR-based model can be used to quickly and inexpensively predict the internal thermal comfort of military camps or other facilities planned to be deployed with ISO 20' containers. It can be used to predict whether or not a facility planned to be deployed with ISO 20' container(s) in a given geographic environment will require an improvement in the thermal comfort of a container (with expensive equipment) before physical deployment of the camp begins. This is a very useful option for practice.

The proposed MLR-based model uses basic environmental parameters to predict the internal temperature, which fits with military reconnaissance -

military meteorology - data, making it easier to use for military camp planning, possibly to be integrated into a specific planning module.

The MLR model has a modelling error of 7.1 % for the ISO standard container building only. As a black-box model, it models the internal temperature of the container by empirically relating external environmental influences without specifying the parameters and structural characteristics of the building on the input side of the model. It is necessary to perform the test for all relevantly different properties and structures of the camp building material.

Based on the results showing the internal temperature modelling of the M63 tent as a camp building material, it can be concluded that the internal temperature of the M63 tent can be accurately described by the MLR-based model. My preliminary assumption was confirmed by the validation, which showed a modelling error of 7.8% for the MLR-based model, which is worse than the 7.1% shown for the ISO 20' container case, but still better than the 14.8% error shown in the previous comparison for the physics-based model. Therefore, the accuracy of the MLR-based model for the M63 sample tent can be considered as very good for general engineering purposes, i.e. suitable for the study and prediction of indoor temperature variation in military field housing unit tents.

4.3   Measuring the impact of elevated CO_2 concentrations in IAQ

The indoor enclosed space is marked by a good quality fresh air with a CO_2 concentration limit of 1000 ppm, or the maximum of 5000 ppm CO_2 allowed by Hungarian and international standards for enclosed comfort spaces. I have also presented the work of HERCZEG (2008) on the assessment of indoor air quality in office spaces, which concludes that the well-being of healthy young people begins to decline significantly after 2 x7 0 minutes in an enclosed space above 3000 ppm CO_2 and 3 x 70 minutes in an enclosed space above 3000 ppm CO_2.

By evaluating the results recorded in my research, I conclude that, in line with the research available in the literature, the performance of soldiers also deteriorates significantly above 3000 ppm concentrations. However, I identify as a new result that, contrary to the literature, the relevant, large deterioration of the effect on military capability does not occur after 3 x 70 min, but already after the first 70 min of loading, because at this point the efficiency of military situational marksmanship capability is reduced by almost half according to our evaluation system. However, after the second 70 min of loading, the performance deterioration was no longer pronounced,

because we can detect a further 5% deterioration of efficiency with the second 70 min of loading, which occurred with the deterioration of execution time.

Taking into account my preliminary measurement results that CO_2 concentrations in ISO 20' containers can reach and exceed 3000 ppm after an hour and a half, special attention must be paid to the provision of fresh air in all military installations where the soldiers' stay is 3 hours (ramp-up time + 70 minutes load) or more. An example is the ISO 20' rest container where, on average, personnel spend 6 hours sleeping in the field.

The results and themes of the research work can be used and extended to special operations training. It may not necessarily be just an ISO 20' container in an interior where 3-4 people are waiting in a relatively small space. For example, in my research work, vehicle interiors and sniper tasks have also arisen, for which the method presented in my research work can be extended to measure the effect of elevated CO_2 concentrations.

4.4 Camp facility IAQ, CO_2 concentration modelling

In the rest areas of a military camp where an ISO 20' container is installed, the CO_2 concentration resulting from the respiration of the occupants is strongly influenced by environmental parameters (pressure difference, wind speed). At present, there are no general mathematical models available that can provide a reliable estimate of the airspace condition based on the size of the ISO 20' container, the filtration characteristic of the container, the external influencing parameters and the point source from the occupant respiration intensity.

In my research, I have proposed and validated a new black-box model to fill the research gaps of such MLR-based models, which represent direct empirical relationships between facility input and output variables.

The proposed MLR-based model is probably the simplest possible black-box type model with very good accuracy, with a deviation (relative) error rate better than 10% on average, as shown in the results section.

Selecting 4+2 different days from a seasonal operation with different ambient and internal temperature ratios and wind speeds proved to be sufficient for the identification to obtain an accurate MLR-based model for a selected season. (If the model is to be applied to the whole year, the identification can easily be performed for each season separately for accuracy). The results confirm the reasonable accuracy of the physics-based

model in the case where the internal field filtration is constant, for which cases research results have been accepted and successfully applied in the literature. The physics and MLR models have been compared. The experiments showed that the MLR-based model predicts the indoor air CO_2 concentration of a camp ISO container with 25% less error than the physically-based model. The proposed MLR-based model is easily identifiable for any given camp placement container building based on the procedure described in the results, making the model general and easily applicable to any camp facility by identifying the input and output variables described in the material and method.

As described above, the proposed MLR-based model has very low equipment/device requirements. Accordingly, only the most basic computing tools are required (e.g. Excel or similar software), which is a great advantage in practice. At the same time, it can be used for quick and inexpensive forecasting of changes in indoor air CO_2 concentrations in military camps or other facilities planned to be deployed with ISO 20' containers, such as whether or not (with expensive equipment) it is necessary to improve the air supply to a container in a planned camp using ISO 20' container(s) in a given geographical environment, before the physical deployment of the camp starts. This is a very useful option for practice.

Further future research could address the refinement of the MLR-based model by splitting a day into several operational cases and/or identifying the model based on several classified days.

The MLR model is not only applicable to comfort spaces, but also to technical areas. Other research could address the modelling of the internal air conditions of fruit and vegetable stores, even combining research on packaging materials and sub-supercritical CO_2 processing, which would make food supply more predictable, safer.

54

5   NEW SCIENTIFIC RESULTS

1. *I conclude that the expected internal temperature - also the recommended design internal temperature - in the housing envelope of military camp conditions with 20' ISO containers in the heating season in the geographical environment of Hungary is higher at $T_b = 24.5 \pm 1$ °C than in built-up residential buildings, which is 22 ± 1 °C.*

   My measurements showed that, based on two years of continuous monitoring, men aged 25-55 years at the 4 borderline bases typically had higher internal temperatures subjectively adjusted for individual thermal comfort.
   According to the measured results, the average internal temperature set for the soldiers' subjective thermal sensation in the camp resting quarters was 24.5 °C. The data were analysed for several subjective thermal comfort settings (90-120 personnel) for a total of one hundred personnel over the entire heating period. By examining the measured data for the whole heating season, as well as by evaluating the data separately for different parts of the heating season - at the beginning of the heating season, in the coldest month of the heating season and at the end of the heating season - I conclude that the set internal temperature of 24.5 ± 1 °C is not only an average value in the camp rest containers constructed from ISO 20' containers, but that the internal temperature of 24.5 ± 1 °C was also generally found separately in the pre- and post-heating season.
   The higher expected temperature is due to a fundamental feature of the ISO standard design. The physical size of the rest enclosure and the resulting thickness of the insulation - 6 cm - and the proximity of the cooling surfaces bordering the enclosure create a feeling of discomfort, which results in a higher internal air temperature setting in cold weather.

2. *I conclude that the variation of the internal temperature of a camp container as a function of external environmental parameters (temperature, wind speed and solar radiation) is described by an MLR-based model with a smaller relative error of $h_t = 7.1\%$ over the measurement range, compared to a physics-based model with $h_t = 14.5\%$.*

The proposed 'black-box' model models the internal temperature of the container by empirically relating the external environmental effects without specifying the parameters and structural characteristics of the building on the input side of the model. Due to simple linear explicit relationships, the MLR-based model has very low equipment/device requirements. Accordingly, only the most basic computing tools are required (e.g. Excel or similar software), which is a great advantage in practice. It can be used for a quick and inexpensive prediction of the internal thermal comfort of a facility to be designed with an ISO 20' container, so that it can be assessed in advance whether or not the thermal comfort of an ISO 20' container in a designed camp facility in a given geographical environment needs to be improved (with expensive equipment) before the physical installation of the camp starts. The parameter values of the MLR-based model presented and proposed in this research work are presented in Table 13.

Table 13, ISO container internal temperature model parameter value

$c_{I,A1}$, m^{2}K/W	0.000153	$c_{v,B}$, Km/s	-0.000429
$c_{k,A1}$, -	0.001046	$c_{b,B}$, -	0.998349
$c_{v,A1}$, Km/s	0.000983	$c_{I,A2}$, m^{2}K/W	0.014592
$c_{b,A1}$, -	0.999045	$c_{k,A2}$, -	0.00178
$c_{I,B}$, m^{2}K/W	0.000007	$c_{v,A2}$, Km/s	0.000076
$c_{k,B}$, -	0.001804	$c_{b,A2}$, -	0.998158

3. *I conclude that the MLR based model describes the change of the internal temperature of the tent M63 as a function of the external environmental parameters (temperature, wind speed and solar radiation) with a relative error of ht = 7.8%. Over the period under study, external parameters, temperature 0 - 35 °C, irradiance 0 - 1000 W/m^2 and wind speed 0-7 m/s.*

The M63 model tent is also important as a camp building material for the construction of temporary facilities for the Hungarian Defence Forces. It is quick to erect, easy to transport and is therefore preferable to ISO 20' containers for short term deployments. It is easy to see that the material of the tent is very different from the structural material of an ISO 20' container and therefore its building physics characteristics are also very different. Therefore, it was not a trivial assumption that the MLR model proposed for modelling the internal

temperature of an ISO 20' container is also suitable for modelling the internal temperature of a M63 container. However, based on the results presented, it can be concluded that the internal temperature of the M63 tent can be accurately described by the MLR-based model. In accordance with my assumptions, as confirmed by the validation results, the modelling error of the proposed MLR-based model is worse than the h_t = 7.1% shown for the ISO 20' container case, but still better than the 14.8% error shown in the previous comparison for the physics-based model. Therefore, the accuracy of the MLR-based model for the M63 tent can be considered as very good. The parameter values of the MLR-based model presented and proposed in this research work are shown in Table 14.

Table 14, Temperature model parameter values for the M63 tent

$c_{I,A1}$, m²K/W	0.000622	$c_{v,B}$, Km/s	-0.001815
$c_{k,A1}$, -	0.005992	$c_{b,B}$, -	0.998772
$c_{v,A1}$, Km/s	-0.013343	$c_{I,A2}$, m²K/W	0.103399
$c_{b,A1}$, -	0.996645	$c_{k,A2}$, -	0.017401
$c_{I,B}$, m²K/W	0.000038	$c_{v,A2}$, Km/s	-0.001037
$c_{k,B}$, -	0.000925	$c_{b,A2}$, -	0.987627

4. *I conclude that after 70 min of indoor air concentration loading above 3000 ppm CO_2, the hit score of the situational shooting effectiveness of military capability decreased and the execution time increased significantly at a significance level of $p \leq 0.005$. Our measurements were performed with subjects aged between 20 and 60 years, with three replicates.*

By evaluating the results recorded in my research, I conclude that, in line with the research available in the literature, the performance of soldiers also deteriorates significantly above 3000 ppm. However, as a new conclusion, it can be identified that, in contrast to the office workers, the large deterioration due to the effect on military performance does not occur after 3 x 70 minutes, but after the first 70 minutes of exposure.

However, after the second 70 min load, the performance degradation was no longer significantly detectable in terms of hit score and hit variance (40 % significance level), but the difference in results recorded after 70 min and 2 x 70 min load was significant at $p \leq 0.025$ significance level (95%).

57

5. *I conclude that the change in CO_2 concentration due to the internal load of a camp container, as a function of external environmental parameters (temperature, wind speed), internal temperature and point source, is described by an MLR-based model with a relative error of $h_t = 9\%$ over the measurement range, taking into account the change in filtration. The carbon dioxide concentrations in the range of 430-5730 ppm, with an external temperature range of 0-35°C and a wind speed range of 0-7 m/s were investigated over the period under study.*

In my research work, I proposed and validated a new black-box model to fill the research gap of MLR-based models that represent direct empirical relationships between external environmental parameters at the facility input and the variable indoor air carbon dioxide concentration at the output. The proposed MLR-based model is probably the simplest possible black-box type model with very good accuracy (better than 90%) based on the results presented. Due to its simple linear, explicit relationships, it has very low equipment/device requirements. Accordingly, only the most basic computational tools are required (e.g. Excel or similar software), so the procedure described in the results can be easily identified for any given military camp accommodation container building, even applied to research on fruit and vegetable storage, whereby not only would human comfort space become more designable, but also food supply in a military camp would become safer. The parameter values of the MLR-based model proposed in this research work are shown in Table 15.

Table 15, CO_2 concentration model parameter values

$c_{K,A1}$, -	0.99659	$c_{K,A2}$, -	0.99847
$c_{\Delta T,A1}$, ppm/°C	-0.80482	$c_{\Delta T,A2}$, ppm/°C	-0.03351
$c_{v,A1}$, ppm s/m	-2.42805	$c_{v,A2}$, ppm s/m	-1.91863
$c_{Kb,A1}$, -	0.00445	$c_{Kb,A2}$, -	0.00142

6 SUMMARY

In the initial phase of my research, I conducted a literature review on several sub-areas, on the definition of baseline data for the application and installation of temporary facilities and on indoor air quality. During the literature search, I found gaps in addition to a lot of useful information, for example, unsatisfactory answers on comfort parameters and energy requirements for non-temporary or not specifically temporary installations. Also not examined were the parameters for determining the technical requirements for the military use of a temporary facility, the construction of a military camp and the level of construction of the associated infrastructure. I could not find any examples of the comfort criteria to be applied to the design requirements and boundary conditions of a military camp.

In my work, I found that the indoor air quality in the rest areas of the campsite is expected to be different in terms of air temperature than that in the built environment. Determining these different requirements is necessary for the design of the utility network of camps designed for long-term occupancy. I have also found that degradation of indoor air quality has a greater impact on military capability than on the performance expected of civilian workers in the average built environment. I conducted the indoor air quality survey using long term outsourced multiple data recordings, and the impact on soldiers was tested using three replicates.

An important finding of the research is that the operational planning of camps designed for military use, to set up operational models, should be defined with parameters that can be directly matched with military reconnaissance (military meteorology) data. In planning operations, it is important to use a common database for the cooperation of the various support and insurance systems, with a view to limiting the amount of data to what is strictly necessary and sufficient. Accordingly, I have sought to find the simplest modelling procedures that meet practical requirements and can be applied with acceptable efficiency in engineering.

In my research on indoor environmental impacts, I not only looked at comfort spaces, but also at logistics buildings and storage facilities. This sub-task, although at first glance it may not seem to be intrinsically related to the topic indicated in the title of the dissertation, had several implications for the research. One of these was the concentration of carbon dioxide in the fresh food (fruit and vegetable) storage at the campsite due to the amount of carbon dioxide produced during fruit respiration, the elevated value of which can be harmful to humans, but can have a positive effect on the shelf life of

fruit and vegetables. Measurements of indoor air quality carbon dioxide concentrations were carried out using several experimental point sources (human, fruit and adjusted food carbon dioxide bottle) with different emission values and several replicates.

On the basis of my research results, I conclude that military camps built using ISO 20' containers should be designed for an internal air temperature of 24.5 ± 1 °C. On the other hand, I propose an MLR-based (Multiple Linear Regression) model that can be used to quickly and inexpensively predict the indoor thermal comfort of military camps or other facilities to be designed and installed with ISO 20' containers. Third, I demonstrate that the proposed MLR black-box model, can be applied to model the internal temperature of the M63 tent. Furthermore, I prove that after 70 minutes of indoor air CO_2 concentration load above 3000 ppm, the efficiency of military capability is significantly reduced, finally, I propose an MLR-based model, which is probably the simplest possible black-box type model that describes with very good accuracy the change of CO_2 concentration inside an ISO 20' container as a function of external environmental influences.

7 KEY PUBLICATIONS RELATED TO THE THESIS

MTMT: https://m2.mtmt.hu/gui2/?type=authors&mode=browse&sel=10074018

Lektorált cikk idegen nyelven:
1. **Patonai Z.,** Kicsiny R., Géczi G. (2022) Multiple linear regression based model for the indoor temperature of mobile containers, HELIYON, https://doi.org/10.1016/j.heliyon.2022.e 12098;
2. **Patonai Z.,** Géczi G. (2021) Research of the internal environment of the military camp buildings, Science, Technology and Innovation, 12 (1): 35–40 doi: 10.5604, ISSN 2544-9125;

Lektorált cikk magyar nyelven:
3. **Patonai Z.,** Géczi G., (2021) Katonai Tábor Élelmiszertárolójának Belső Levegőminőség Vizsgálata, Acta Agronomica Óváriensis Vol. 62. Különszám I.: 97–109, Mosonmagyaróvár
4. **Patonai Z.,** Géczi G., Kicsiny R., Baráth I. (2020) Katonai tábori elhelyezés, belső környezet Katonai Logisztika 2020. évi 3. szám, DOI: 10.30583/2020.3.045, e-ISSN 1789-6398, ISSN 1588-4228 (https://www.mkle.net/products/a2020-3-szam/)
5. **Patonai Z.,** Géczi G. (2018) Tábori elhelyezésnél alkalmazott konyhatechnológiák bemutatása, Katonai Logisztika 2018. évi 3-4. szám, DOI: 10.30583/2018/3-4/123, e-ISSN 1789-6398, ISSN 1588-4228 (https://www.mkle.net/products/a2018-evi-3-4-szam/)
6. **Patonai Z**., (2018) Tábori elhelyezésnél alkalmazott fűtési rendszerek, Haditechnika folyóirat - 2018/3. szám - HU ISSN 0230-6891 (https://haditechnikaiintezet.hu/magazin/haditechnika-20183)

Idegen nyelvű konferencia kiadvány
7. **Patonai Z**., Géczi G., (2021): Research of the internal environment of the military camp buildings, Risk factors of food chain, XXIst International Scientific Conference, Poland, Iwonicz, 06-08, of September 2021, p. 40-41., ISBN 978-963-269-775-8
8. **Patonai Z**., Kicsiny R., Géczi G. (2021): Research of the internal environment of the military camp buildings, Book of Abstracts: Efficiency, solar and thermal energy for the human comfort. Hungarian University of Agriculture and Life Science, Gödöllő. ISBN 978-963-269-958-5